

# TOWARDS EFFICIENT AND SCALABLE MULTI-AGENT REASONING VIA BAYESIAN NASH EQUILIBRIUM

Anonymous authors

Paper under double-blind review

## ABSTRACT

Large Language Models (LLMs) exhibit strong reasoning capabilities, which can be further enhanced through multi-agent frameworks. However, existing multi-agent methods often suffer from high computational costs and lack theoretical convergence guarantees. To address these limitations, we introduce an incomplete information perspective to enhance the scalability of multiple LLMs by modeling them with Bayesian Nash Equilibrium (BNE) and propose Efficient Coordination via **Nash** Equilibrium (EcoNash), a hierarchical reinforcement learning framework. EcoNash guides multiple LLMs to achieve BNE by integrating distributed reasoning and centralized commitment, ensuring that each LLM independently generates optimal answers based on its own beliefs without the need for extensive inter-agent communication. Theoretically, we prove that our framework achieves a regret bound of  $O(N\sqrt{T}/1-\gamma)$ , which grows sublinearly with  $T$ , while multi-agent frameworks that do not attain BNE can at best achieve  $O(\delta_{\max} T/1-\gamma)$ . Empirically, our method outperforms single-LLM approaches by 10.9% and surpasses existing multi-LLM methods by 11.2% over six benchmark tests covering complex reasoning and planning tasks on average. Additionally, scalability experiments show that our approach efficiently integrates more models, confirming its flexibility and scalability, potentially leading to larger multi-LLM ensembles.

## 1 INTRODUCTION

Large Language Models (LLMs) (Brown et al., 2020) have demonstrated exceptional reasoning capabilities across various tasks, including natural language understanding, generation, and complex problem-solving. Recent research enhances their reasoning abilities by exploring multi-agent frameworks (Du et al., 2024; Chan et al., 2024; Liang et al., 2023; Chen et al., 2023; Hong et al., 2023) where multiple LLMs collaborate. These frameworks simulate human-like discussions, boosting diversity and creativity and potentially yielding more robust solutions in real-world applications.

However, existing multi-agent frameworks are computationally expensive, as they require multiple model instances and repeated rounds of interaction (Wu et al., 2023). Agents must read and process one another’s outputs, increasing communication overhead and latency. Adding components such as judges or verifiers further compounds the problem by introducing more computational layers (Zheng et al., 2023). What’s more, the current multi-agent debate (MAD) systems lack theoretical guarantees for convergence(Du et al., 2024), while MAD between LLMs can be viewed as games that need to converge to a single, stable solution. While empirical results may demonstrate convergence in certain cases, the introduction of a judge can further guide the debate direction(Lu et al., 2024), the lack of solid theoretical foundations leaves the reliability and stability of such systems uncertain.

To address the above challenges, we propose a novel framework called *EcoNash* (Efficient Coordination via *Nash* Equilibrium), which introduces a *Bayesian Nash Equilibrium (BNE)* perspective to multi-LLM systems. Inspired by reinforcement learning, our framework constructs a hierarchical coordination mechanism. Each Execution LLM operates independently with its own belief network, receiving only the question and strategy from the Coordinator LLM. This enables multiple Execution LLMs to engage in distributed reasoning, guided by the Coordinator LLM, to achieve BNE by optimizing the belief network and belief encoder. Optimization employs adaptive rewards and an early stopping criterion. When the outputs of the Execution LLMs consistently meet convergence metrics, the system is considered to have reached an approximate BNE, and further iter-

054      ations are halted. This approach not only reduces unnecessary computations but also minimizes the  
 055      input tokens required by the Coordinator LLM, enhancing overall efficiency. Unlike existing meth-  
 056      ods, Execution LLMs can generate outputs in parallel without the need for extensive inter-agent  
 057      communication in EcoNash, reducing both communication costs and computational overhead.

058      Theoretically, we demonstrate that EcoNash achieves a regret bound of  $O(N\sqrt{T}/1-\gamma)$ , which grows  
 059      sublinearly with  $T$ . In contrast, multi-agent frameworks that do not attain BNE can at best achieve a  
 060      regret bound of  $O(\delta_{\max}T/1-\gamma)$ . Our framework’s convergence toward BNE provides strong theoret-  
 061      ical guarantees for efficiency, while inference incurs lower consumption costs than existing multi-  
 062      LLM systems, providing significant insights for scaling up multi-LLM systems. Based on it we  
 063      verify whether EcoNash can address scalability, a challenge often overlooked in prior works (Wu  
 064      et al., 2024; Yin et al., 2023; Lan et al., 2024; Yuan et al., 2024a). By constructing a Coordinator-  
 065      Execution subsystem based on local Nash equilibria, we scale EcoNash to a larger LLMs ensemble  
 066      framework (Central-Coordinator-Execution) in global Nash, resulted in enhanced performance.

067      Through extensive experiments on six benchmarks, including complex reasoning and planning tasks,  
 068      our method outperforms single-agent approaches by 10.9% and surpasses the performance of ex-  
 069      isting multi-agent methods by 11.2% in average, confirming the robustness and efficiency of our  
 070      framework. Scalability experiments further demonstrate that EcoNash effectively integrates numer-  
 071      ous models, showcasing its applicability in large-scale settings. When the number of Execution  
 072      LLMs is increased to nine, performance improves by 18.1% compared to three Execution LLMs.

073      We summarize our major contributions as follows:

- We conceptually formalize BNE in multi-LLM systems and technically instantiate it through a hierarchical optimization framework *EcoNash* to improve reasoning over collaboration of LLMs.
- We address the non-trivial challenge of scaling up multi-LLM systems with local-global Nash, facilitated by EcoNash’s low reliance on inter-agent communication and convergence guarantee.
- Extensive experiments on six benchmarks demonstrate that EcoNash outperforms existing single- and multi-agent methods, while scalability experiments confirm its ability to efficiently integrate numerous models for large-scale settings, potentially leading to larger multi-LLM ensembles.

## 083      2 RELATED WORK

085      **Prompting Large Language Models to Reason.** Large language models are significantly more  
 086      capable of complex reasoning with the advancement of prompt techniques (Wei et al., 2022; Kojima  
 087      et al., 2022; Wang et al., 2023; Yao et al., 2023; Chia et al., 2023; Fu et al., 2022; Wan et al.,  
 088      2023; Zhang et al., 2023b; Zhou et al., 2022). Wei et al. (2022) introduced Chain-of-Thought (CoT)  
 089      prompting, which presents step-by-step reasoning examples within the prompt. This enables the  
 090      model to engage in explicit reasoning, enhancing its ability to follow the logical progression that  
 091      leads to the correct answer. Various extensions of CoT have been developed to improve reasoning  
 092      performance further. Zero-shot CoT (Kojima et al., 2022) eliminates the need for manually con-  
 093      structing exemplars, prompting models with phrases like “Let’s think step by step” to encourage  
 094      reasoning. Wang et al. (2023) proposed self-consistency (SC) sampling, where multiple reasoning  
 095      paths are sampled, and the final answer is determined by majority voting. To enable LLMs to engage  
 096      in deliberate decision-making, Tree of Thoughts (ToT) Yao et al. (2023) generates multiple potential  
 097      answers at each reasoning step, building a tree of possible solutions. It then applies breadth-first or  
 098      depth-first search to navigate the tree, ultimately determining the rationale and final answer.

099      **Multi-agent Debate for Large Language Models Reasoning.** Various multi-agent debate strate-  
 100      gies(Du et al., 2024; Chan et al., 2024; Liang et al., 2023; Chen et al., 2023; Smit et al., 2024; Zhang  
 101      et al., 2023a; Pham et al., 2023) have been developed to strengthen the reasoning ability of LLMs  
 102      further. Du et al. (2024) introduced an approach where multiple instances of LLMs propose their  
 103      individual reasoning processes, engaging in multiple rounds of debate to reach a consensus on the  
 104      final answer. This method not only significantly enhances reasoning performance across a variety  
 105      of tasks but also reduces the occurrence of hallucinations. Some studies(Chan et al., 2024; Liang  
 106      et al., 2023) incorporate role-playing into multi-agent debate strategies using role-specific prompts,  
 107      which foster divergent thinking and enhance the reasoning capabilities of LLMs. However, cur-  
 108      rent multi-agent debate strategies face high computational costs and lack theoretical guarantees for  
 109      convergence. In this work, we introduce an incomplete information perspective to enhance the scal-

ability of multiple LLMs to ensure independent reasoning by each Execution LLM while addressing communication cost. Our framework ensures convergence through rigorous theoretical analysis.

### 3 METHOD

In this section, we develop a theoretical framework for multi-LLM systems to achieve BNE. We begin by defining and establishing the implementation of BNE within a multi-LLM system (Section 3.1). We conduct a convergence analysis and evaluate regret bounds to demonstrate the efficiency of our method (Section 3.2). Then, we outline our optimization approach with prompt embeddings (Section 3.3), integrating both inference and optimization processes in Section 3.3 , followed by our scaling-up method to enhance the framework’s scalability in Appendix A.4).

#### 3.1 BAYESIAN NASH EQUILIBRIUM IN THE MULTI-LLM FRAMEWORK

##### 3.1.1 DEFINITION AND IMPLEMENTATION OF BNE

A **Bayesian Nash Equilibrium** (BNE) is a strategy profile where each agent maximizes its expected utility based on its beliefs about other agents’ strategies. In the context of incomplete information games, where each LLM does not have direct access to the outputs of other LLMs, we construct a hierarchical framework consisting of execution LLMs and a coordinator LLM to establish the game. The coordinator LLM takes a question as input and outputs corresponding strategy and format specifications to guide execution LLMs. After receiving answers from execution LLMs, it generates a final commitment to address the question. Each execution LLM maintains its belief state  $\mathbf{b}_i \in \mathbb{R}^d$  and receives observations  $O_i = [e_t, e_s, \mathbf{b}_i]^\top$ , where  $e_t$  encodes the task and  $e_s$  represents the coordinator’s strategy. To enable coordination without direct information sharing, we implement a belief network  $B_i(\tau_i, O_i; \theta_i^B)$  that updates each agent’s state based on its history  $\tau_i$  and current observation, generating prompt embeddings  $\mathbf{e}_i$ . A belief encoder  $f_e(\{\mathbf{b}_i\}_{i=1}^N; \theta_e)$  then aggregates these beliefs into group information  $\mathbf{E}$ , and then the centralized mixing network of coordinator LLM processes this group information to guide coordination through a commitment  $C$ .

To quantify the effectiveness of different belief states, we employ Q-functions  $Q_i(O_i, \mathbf{e}_i; \theta_i^B)$  that evaluate prompt embeddings generated by the belief network. These value estimates guide the optimization of belief network parameters  $\theta_i^B$ . A BNE is achieved when each agent’s belief network parameters generate prompt embeddings that maximize its expected utility:

$$\mathbf{e}_i^* = \arg \max_{\mathbf{e}_i} \mathbb{E}_{\mathbf{E} \sim f_e(\{\mathbf{b}_j\}_{j=1}^N; \theta_e)} [U_i(O_i, \mathbf{E}, \mathbf{e}_i)].$$

To guarantee the existence of BNE, the following conditions need to be established:

- **Compactness and Convexity:** For each agent  $i$ , the mixed strategy space  $\Pi_i$  is non-empty, compact, and convex, consisting of all mappings from types  $\Theta_i$  to probability distributions.
- **Continuity:** The payoff function  $U_i(\theta, a)$  is continuous in the type profile and the action profile.
- **Quasi-Concavity:** For each agent  $i$ , the expected payoff is quasi-concave in  $a_i$  for fixed  $\theta_i$ .

Under these conditions, we can apply Glicksberg’s Fixed Point Theorem (Ahmad et al., 2023) to guarantee the existence of BNE. Specifically, the best response correspondences  $BR_i(\pi_{-i})$  for each agent  $i$  are non-empty, convex-valued, and upper hemicontinuous.

**Theorem 1** (Existence of Bayesian Nash Equilibrium). *In the multi-agent LLM framework with the specified conditions, there exists a Bayesian Nash Equilibrium strategy profile  $\bar{\pi}^* = (\pi_1^*, \pi_2^*, \dots, \pi_N^*)$  such that no agent can unilaterally deviate to improve its expected payoff, given its beliefs about other agents’ types and strategies. For the proof, please refer to Appendix A.1.*

**Proposition 1** (Convergence to Bayesian Nash Equilibrium). *Under appropriate assumptions about the learning rate, exploration strategy, and Q-network properties, the prompt embedding adjustment via TD loss converges to a Bayesian Nash Equilibrium. The proof is provided in Appendix A.2.*

#### 3.2 CONVERGENCE ANALYSIS AND BAYESIAN REGRET BOUND

In this section, we analyze the convergence properties of our EcoNash framework through Bayesian regret. Our analysis demonstrates that the framework’s belief network structure and coordinated learning process lead to efficient convergence toward BNE, achieving sublinear regret bound  $O(N\sqrt{T}/1-\gamma)$  in contrast to the linear regret of existing multi-agent debate methods.

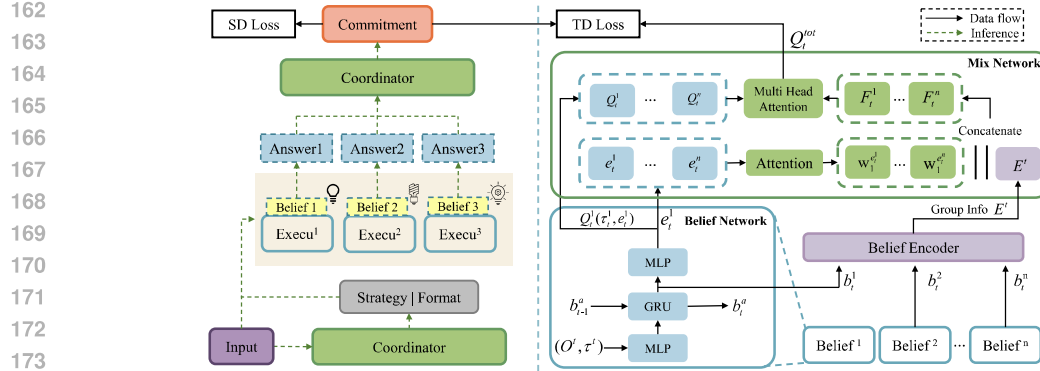


Figure 1: The EcoNash framework. The inference procedure is shown by green arrows: the coordinator receives the question, provides a strategy to the Execution LLM, which outputs an answer. Afterwards, the coordinator forms the final commitment. Simultaneously, the Execution LLM passes its belief to the belief encoder, embedding agent information. TD Loss updates the belief network, and SD Loss updates the belief encoder, optimized to achieve BNE, as the red gradient flow.

For each agent  $i$ , we measure the learning efficiency using Bayesian regret over  $T$  steps:  $R_i(T) = \mathbb{E}_{s_t, \pi_t} \left[ \sum_{t=1}^T (V_i^*(s_t) - V_i^{\pi_t}(s_t)) \right]$ , where  $V_i^*(s)$  represents the optimal value under BNE policies and  $V_i^{\pi_t}(s)$  is the value under current policies at time  $t$ . The expectation accounts for randomness in both state transitions and policy choices. To analyze the total Bayesian regret  $R(T) = \sum_{i=1}^N R_i(T)$ , we make standard assumptions (see Appendix A.3) to propose Lemma 1, and we prove Lemma 1 in B.1. Using Lemma 1 we bound the Bayesian regret and provide a proof sketch here, with detailed proofs and comparison with multi-agent debate in Appendix B.2 and B.3.

**Lemma 1** (Performance Difference). *For joint policies  $\pi = (\pi_i, \pi_{-i})$  and  $\pi' = (\pi'_i, \pi'_{-i})$ , the value difference for agent  $i$  is:*

$$V_i^{\pi'}(s) - V_i^{\pi}(s) = \frac{1}{1-\gamma} \mathbb{E}_{s \sim d_{\pi'}} [\mathbb{E}_{a \sim \pi'} Q_i^{\pi}(s, a) - \mathbb{E}_{a \sim \pi} Q_i^{\pi}(s, a)],$$

where  $d_{\pi'}$  is the state distribution under  $\pi'$ , and  $a = (a_i, a_{-i})$  denotes joint actions.

Applying this lemma to our regret analysis yields (Jin et al., 2020; Fujimoto et al., 2018):

$$R(T) = \sum_{i=1}^N \frac{1}{1-\gamma} \mathbb{E}_{s_t, \pi_t} \left[ \sum_{t=1}^T (\mathbb{E}_{a_t^* \sim \pi^*} Q_i^{\pi_t}(s_t, a_t^*) - \mathbb{E}_{a_t \sim \pi_t} Q_i^{\pi_t}(s_t, a_t)) \right]$$

where  $\pi^*$  represents the BNE policies. Through analysis of estimation error  $\epsilon_t$  and policy suboptimality  $\delta_t$ , we establish:  $\mathbb{E}_{a_t^* \sim \pi^*} Q_i^{\pi_t}(s_t, a_t^*) - \mathbb{E}_{a_t \sim \pi_t} Q_i^{\pi_t}(s_t, a_t) \leq 2\epsilon_t + \delta_t$ . This leads to:

$$R(T) \leq \sum_{i=1}^N \frac{1}{1-\gamma} (2C_\epsilon + C_\delta) \sum_{t=1}^T \frac{1}{\sqrt{t}} = O\left(\frac{N\sqrt{T}}{1-\gamma}\right).$$

### 3.3 FRAMEWORK OF ECONASH

In this section, we present a framework designed to achieve BNE within a multi-LLMs system, satisfying the assumptions in Appendix A.3 to enable Lemma 1 can be applied to analyze its Bayesian regret. The framework has two primary phases: **Inference** and **Optimization**. The inference phase involves generating and propagating strategies and responses, while optimization phase focuses on updating strategies to align with global objectives and optimizes their beliefs to achieve BNE.

#### 3.3.1 INFERENCE PHASE

During the inference phase, a Coordinator LLM generates an informative strategy and a format based on the input question  $q$ . These are then disseminated to the Execution LLMs, which independently produce their respective answers. Finally, the Coordinator LLM aggregates these answers to form a final commitment, detailed inference flow as illustrated clearly in Figure 1: the green inference flow.

216    3.3.2 OPTIMIZATION PHASE  
 217

218    The optimization phase of EcoNash implements a hierarchical learning framework under the cen-  
 219    tralized training with decentralized execution (CTDE) paradigm(Foerster et al., 2018b; Kraemer &  
 220    Banerjee, 2016), satisfying our theoretical assumptions while optimizing towards the Bayesian Nash  
 221    Equilibrium (BNE). Under Assumption 2, execution LLMs aim to align with posterior distributions  
 222    determined by the coordinator LLM, achieved through our belief network architecture. The game  
 223    regularity (Assumption 3) ensures stable information gain across timesteps, guiding our design of the  
 224    belief encoder. The concentrability condition (Assumption 4) bounds the error in value estimation,  
 225    informing our mixing network structure. The optimization procedure is summarized in Algorithm 1.  
 226

227    REWARD SETTING    The reward function  $R$  is central to the optimization stage, providing feedback  
 228    on each agent’s performance. Multiple types of rewards are designed to capture different aspects of  
 229    performance. The Action Likelihood Reward evaluates the consistency of an agent’s actions with  
 230    the commitment  $C$ , inspired by maximum entropy inverse reinforcement learning (Zhu et al., 2023).  
 231    Task-specific rewards address correctness in tasks like math problem solving or relevance in plan-  
 232    ning (Hao et al., 2023). The Self-Evaluation Reward enables the coordinator to assess the quality  
 233    of generated answers, promoting coherence, consistency, and creativity across agents, driving optimi-  
 234    zation toward BNE (Xie et al., 2024b). More details are provided in Appendix B.4.  
 235

236    INDIVIDUAL BELIEF NETWORK    Execution  $i$  employs a belief network  $B_i(\tau_i, O_i; \theta_i^B)$  to update  
 237    its belief state  $\mathbf{b}_i$  based on its history trajectory  $\tau_i$  and current observation  $O_i$ . The belief state  $\mathbf{b}_i$  is  
 238    used to adjust the prompt embedding  $\mathbf{e}_i = [T_i, p_i]$ , which defined as:

$$239 \quad T_i = T_{\min} + (T_{\max} - T_{\min}) \cdot \sigma(W_T \mathbf{b}_i + b_T), \quad p_i = p_{\min} + (p_{\max} - p_{\min}) \cdot \sigma(W_p \mathbf{b}_i + b_p),$$

240    with  $\sigma(\cdot)$  as the sigmoid activation function. Here,  $T_i$  adjusts the softmax distribution, and  $p_i$  sets  
 241    the sampling threshold. The belief network outputs the prompt embedding  $\mathbf{e}_i$  and Q-value  $Q_i^t$  for  
 242    the mixing network, while passing  $\mathbf{b}_i$  to the belief encoder for group-level dynamics. It is optimized  
 243    using the TD loss, where  $r_i^t$  is the local reward and  $\phi$  denotes the parameters of the Q-value function:

$$244 \quad \mathcal{L}_{\text{TD}}^i(\theta_i^B) = \mathbb{E}_{\mathcal{D}} \left[ \left( r_i^t + \gamma \max_{\mathbf{e}_i^{t+1}} Q_i^{t+1}(\tau_i^{t+1}, \mathbf{e}_i^{t+1}; \phi') - Q_i^t(\tau_i^t, \mathbf{e}_i^t; \phi) \right)^2 \right],$$

245    BELIEF ENCODER    The belief encoder  $f_e(\cdot; \theta_e)$  aggregates the belief states from all agents  
 246    to generate a group-level representation  $\mathbf{E} = f_e(\{\mathbf{b}_i\}_{i=1}^N; \theta_e)$ . using multi head atten-  
 247    tion with  $H$  attention heads to capture inter-agent relationships. Each head is computed  
 248    as  $\text{head}_h = \text{Attention}(W_h^Q \mathbf{b}, W_h^K \mathbf{b}, W_h^V \mathbf{b})$ , and the final output is obtained by  $\mathbf{E} =$   
 249     $\text{Concat}(\text{head}_1, \dots, \text{head}_H)W_h^O$ , with  $W_h^Q, W_h^K, W_h^V$  being learnable parameters, and  $W_h^O$  is the out-  
 250    put projection matrix. The belief encoder is optimized as:  $\mathcal{L}_e(\theta_e) = \mathcal{L}_{\text{TD}}^{\text{tot}}(\phi) + \lambda_e \sum_i \mathcal{L}_{\text{TD}}^i(\theta_i^B)$ .  
 251

252    CENTRALIZED MIXING NETWORK    The Centralized Mixing Network is designed to coordinate  
 253    belief information from execution LLMs, facilitating optimization towards BNE. Prompt embed-  
 254    dings  $\{\mathbf{e}_i^t\}_{i=1}^N$  are processed via self-attention to capture intra-agent dependencies, producing trans-  
 255    formed embeddings  $\{\mathbf{w}_i^t\}_{i=1}^N$ . These embeddings are concatenated with the group-level representa-  
 256    tion  $\mathbf{E}^t$  to generate feature transformations  $\{F_i^t\}_{i=1}^N$ , encoding both local agent-specific and global  
 257    group-level information. The feature transformations  $\{F_i^t\}_{i=1}^N$  and individual Q-values  $\{Q_i^t\}_{i=1}^N$   
 258    are then combined via multi-head attention to compute the global value function  $Q_{\text{tot}}^t$ , capturing  
 259    complex local-global interactions. The network is optimized by minimizing the composite loss:  
 260     $\mathcal{L}_{\text{mix}}(\phi) = \mathcal{L}_{\text{TD}}^{\text{tot}}(\phi) + \mathcal{L}_{\text{SD}} + \lambda_m \sum_i \|Q_i^t - Q_{\text{tot}}^t\|^2$ , where the TD loss aligns  $Q_{\text{tot}}^t$  with  $r_{\text{tot}}$ :  
 261

$$262 \quad \mathcal{L}_{\text{TD}}^{\text{tot}}(\phi) = \mathbb{E}_{\mathcal{D}} \left[ \left( r_{\text{tot}} + \gamma \max_{\{\mathbf{e}_i^{t+1}\}} Q_{\text{tot}}^{t+1}(\tau_{t+1}, \{\mathbf{e}_i^{t+1}\}; \phi') - Q_{\text{tot}}^t(\tau_t, \{\mathbf{e}_i^t\}; \phi) \right)^2 \right],$$

263    with  $\tau_t = \{O_i^t\}_{i=1}^N$  representing the joint observations, and  $\{\mathbf{e}_i^t\}_{i=1}^N$  as the agents’ belief embed-  
 264    dings. The similarity difference (SD) loss aligns the feature transformations  $\{F_i^t\}_{i=1}^N$  with the coor-  
 265    dinator LLM’s commitment  $C$ :  $\mathcal{L}_{\text{SD}} = \lambda_b \sum_i (1 - \text{sim}(F_i^t, C))^2$ . A consistency term further ensures  
 266     $Q_i^t$  aligns with  $Q_{\text{tot}}^t$ . The target parameters  $\phi'$  are updated via a soft update rule:  $\phi' \leftarrow \tau \phi + (1 - \tau) \phi'$ ,

270 where  $\tau$  is the update rate. By synthesizing belief information and aligning with  $C$ , the mixing network ensures monotonicity, guaranteeing that improvements in individual agent performance positively impact global coordination, enabling stable convergence to the equilibrium. The detailed proof of monotonicity can be found in Appendix A.5.

271  
 272  
 273  
 274  
 275 **EARLY STOPPING** To ensure efficient optimization and convergence to stable solutions, early stopping is implemented based on three key criteria. First, Commitment Stability is achieved when the change in the coordinator’s commitment satisfies  $\|\Delta C\| = \|C_{t+1} - C_t\| \leq \epsilon_C$ . Second, Reward Convergence is monitored such that the average reward across agents reaches a predefined threshold,  $\frac{1}{N} \sum_{i=1}^N r_i \geq R_{\text{threshold}}$ . Lastly, Loss Convergence is ensured when the total loss stabilizes, satisfying  $|L_{\text{tot}}^{t+1} - L_{\text{tot}}^t| \leq \epsilon_L$ , where  $L_{\text{tot}}$  is the sum of individual agent losses  $\sum_i L_i$ , execution loss  $L_e$ , and the mixing loss  $L_{\text{mix}}$ . These criteria comprehensively monitor the optimization process, ensuring both strategic alignment and task performance while preventing premature termination.

---

**Algorithm 1** Optimization Phase of EcoNash
 

---

284  
 285 **Require:** Execution LLMs  $\{\text{ExecLLM}_i\}$ , Coordinator LLM, Networks  $\{f_e, f_{\text{mix}}\}$   
 286 **Require:** Thresholds  $\{\epsilon_C, R_{\text{threshold}}, \epsilon_L\}$ , Maximum episodes  $T_{\max}$   
 287 **Ensure:** Optimized network parameters  
 288 1: **while** not converged and  $t < T_{\max}$  **do**  
 289   2: // Parallel execution and local optimization for each agent  
 290   3: **for** each Execution LLM  $i$  **do**  
 291     4: Update belief state  $b_i$  and generate output  $u_i$  ▷ Run execution LLM  
 292     5: Compute rewards:  $r_i \leftarrow \alpha_1 r_i^{\text{AL}} + \alpha_2 r_i^{\text{TS}} + \alpha_3 r_i^{\text{SE}}$  ▷ Action likelihood + Task +  
 293       Self-evaluation  
 294     6: Store transition  $(O_i, u_i, r_i, O'_i)$  in replay buffer  $\mathcal{D}$   
 295     7: Update individual belief network parameters ▷ Using TD loss  
 296   8: **end for**  
 297   9: // Global coordination and optimization  
 298   10: Update belief encoder  $f_e$  ▷ Using global TD loss + local TD losses  
 299   11: Update mixing network  $f_{\text{mix}}$  ▷ Using TD + similarity + consistency losses  
 300   12: Get new commitment  $C_{t+1}$  from Coordinator  
 301   13: // Check convergence conditions  
 302   14: **if**  $\|C_{t+1} - C_t\| \leq \epsilon_C$  **and**  $R_{\text{avg}} \geq R_{\text{threshold}}$  **and**  $|L_{\text{tot}}^{t+1} - L_{\text{tot}}^t| \leq \epsilon_L$  **then**  
 303     15:   **break** ▷ Early stopping when all criteria are met  
 304   16: **end if**  
 17: **end while**

---

## 4 EXPERIMENT

305 In this section, we present the experiment setup in Section 4.1, demonstrate the performance against  
 306 baseline methods in Section 4.2, validate the heterogeneous results of different models in Section 4.3, test scale-up capability in Section 4.4, and conduct ablation studies in Section 4.5.

### 4.1 SETUPS

312 **Models and Datasets.** We evaluate 4 newly released opensourced LLMs: LLaMA3.1  
 313 8B (Dubey et al., 2024), LLaMA3.1 70B, Mistral-7B (Jiang et al., 2023), LLaMA3.1 405B  
 314 across 5 reasoning tasks, including 4 mathematical tasks (GSM8K (Cobbe et al., 2021), GSM-  
 315 Hard (Gao et al., 2023), MATH (Hendrycks et al., 2021), SVAMP (Patel et al., 2021)) and one  
 316 commonsense reasoning task (StrategyQA (Geva et al., 2021)). Then, we evaluate the most pow-  
 317 erful LLM (GPT4 turbo) in a very challenging planning task (Travelplanner (Xie et al., 2024a)) to  
 318 further validate the performance. The details of evaluation tasks can be found in Appendix B.5.

319 **Compared Methods and Evaluation Metrics** We compare EcoNash against several strong base-  
 320 line types widely adopted: (i) single-round CoT prompting, including zero-shot and few-shot  
 321 CoT (Kojima et al., 2022; Wei et al., 2022); (ii) multi-round CoT prompting, Self Consistency  
 322 SC (Wang et al., 2023) method, where we sample answers 64 times and employ majority voting  
 323 for answer selection; (iii) value-guided search approaches with learned action-value functions, in-  
 cluding TS-LLM (Feng et al., 2023) which leverages AlphaZero-style value networks for MCTS,

and PPO-MCTS (Liu et al., 2024) which learns value models to evaluate generation quality in tree search; (iv) multi-round self-improving approaches, using ToT (Yao et al., 2023), RAP (Hao et al., 2023) and React(Yao et al., 2022) as baselines, with BFS and MCTS for tree search, respectively, following their original implementations for answer selection; and (v) multi-LLM reasoning frameworks, including rStar (Qi et al., 2024) and multi-agent debate (Du et al., 2024).

**EcoNash Setups** In this section, the EcoNash framework includes one coordinator and three Execution LLMs. The hyperparameters for training can be found in Appendix B.6. To ensure a fair comparison with the baseline, we use four identical models for these LLMs. For heterogeneous results, we also evaluate EcoNash with different models in Table 3. All evaluations are conducted in a zero-shot setting, with a general prompt provided in Appendix C. Notably, while we set a 50-token constraint for the coordinator’s strategy generation, considering that LLMs may not strictly follow length instructions (Yuan et al., 2024b), who showed that 95% of responses stay within  $1.4 \times$  and 50% within  $1.0 \times$  of the specified length, we implement a 70-token hard cutoff with regeneration mechanism, which effectively controls the token usage as verified in Table 4.

## 4.2 MAIN RESULT

Table 1 shows a detailed comparison of each method on four mathematical and one commonsense reasoning dataset. Empirical results demonstrate that EcoNash outperforms most baselines across all complex reasoning benchmarks. On average, EcoNash outperforms the single-round method Zero-shot CoT by 25.6%, Few-shot CoT by 6.3%, multi-round CoT prompting SC by 10.9%, multi-round self-improving approaches ToT by 11.2%, multi-LLM reasoning frameworks rStar by 6.4%.

Furthermore, when evaluated on the very challenging Travelplanner benchmark using GPT-4-Turbo in Table 2, EcoNash enhanced the final pass rates to 7.2% on the validation set and 9.3% on the test set, while compared to 2.3% and 3.7% achieved by a three-round multi-agent debate approach.

These results demonstrate that EcoNash effectively leverages the capabilities of more powerful models and outperforms alternative reasoning optimization methods in complex tasks. Additionally, we provide a corresponding example for MATH which are available in Appendix D. Note that EcoNash uses fewer tokens compared to multi-round CoT prompting SC, multi-round self-improving approaches ToT, and Multi-Agent Debate, meanwhile achieved performance improvements.

## 4.3 ADDITIONAL RESULT

To evaluate the impact of both the Coordinator LLM and Execution LLM performance on the EcoNash framework and find whether heterogeneous Execution LLMs can also achieve a BNE, we conducted two types of experiments: one pairing a strong Coordinator LLM with weaker Execution LLMs, and another pairing a weak Coordinator LLM with stronger Execution LLMs. These experiments were further divided into homogeneous and heterogeneous execution groups for detailed analysis. To ensure a fair comparison, the Coordinator LLM was consistently set to Llama3.1 70b across all experiments. For the heterogeneous execution group, we used the following configurations: Llama 3.1 8b, Llama 3 8b, and Mixtral 7b, as well as another configuration consisting of Mixtral 8x22b, Qwen1.5 110b, and Llama3.1 405b. For the homogeneous execution group, two configurations were tested: one with three weak models Llama 3.1 8b, and another with three strong models Llama 3.1 405b. Experimental results indicate that stronger Execution LLMs improve performance by providing higher-quality answers and achieving BNE more efficiently. Additionally, heterogeneous model perform worse than homogeneous models due to increased challenges in reaching BNE, but still outperform baseline method Few-shot CoT .

To assess the cost efficiency of the EcoNash framework, Table 4 presents the average token usage of EcoNash, Multi-Agent Debate, RAP, and Self Consistency (SC) across the Math, GSM8K, and GSM-Hard datasets for three models: Llama 3.1 70B, Mixtral 8x7B, and Mixtral 8x22B. The results demonstrate that EcoNash reduces token consumption by an average of 21.4% compared to Multi-Agent Debate (3 rounds). Notably, when the Coordinator LLM provides detailed strategies with answer(as shown in the token consumption data in Table 4), token usage increases an average of 112% higher token consumption as each Execution LLMs must process the full strategy.

## 4.4 SCALE UP RESULT

We analyzed the impact of varying the number of agents further to validate EcoNash across a broader range of LLMs. We conducted three sets of experiments on the MATH, GSM-Hard, SVAMP, and

378 Table 1: Empirical results of five reasoning datasets: GSM8K, GSM-Hard, SVAMP, Strategy QA,  
 379 MATH. **Bold** face numbers indicate the best performance, while underline means the second best.

381	Dataset	Method	Mistral-8×7B	Mistral-8×22B	LLaMA3.1-70B	LLaMA3.1-405B	Average
382	GSM8K	Zero-shot CoT	62.06	72.14	78.38	86.40	74.74
383		Few-shot CoT	74.92	84.05	95.10	<u>96.80</u>	<b>87.71</b>
384		SC@maj64	71.08	<u>86.24</u>	89.56	92.40	84.82
385		rStar	<u>75.82</u>	81.92	91.13	94.16	85.76
386		ToT	71.46	82.60	84.52	92.73	82.83
387		RAP	72.03	76.97	81.33	92.14	80.62
388		TS-LLM	74.21	84.68	<u>94.82</u>	96.42	87.53
389		PPO-MCTS	73.45	82.76	92.24	94.85	85.83
390		EcoNash	<b>76.97</b>	<b>88.20</b>	<b>96.70</b>	<b>98.80</b>	<b>90.17</b>
391	GSM-Hard	Zero-shot CoT	21.47	32.24	36.78	42.17	33.17
392		Few-shot CoT	26.71	41.35	45.21	52.88	41.54
393		SC@maj64	22.47	<u>44.19</u>	39.76	47.39	38.45
394		rStar	20.21	37.91	<u>49.82</u>	52.75	40.17
395		ToT	24.39	41.71	37.25	46.84	37.58
396		RAP	22.47	42.79	38.97	46.44	37.67
397		TS-LLM	<b>26.85</b>	42.92	47.76	<u>55.24</u>	<b>41.69</b>
398		PPO-MCTS	24.86	40.12	44.53	53.42	40.73
399		EcoNash	<u>25.76</u>	<b>47.58</b>	<b>51.43</b>	<b>60.10</b>	<b>46.22</b>
400	SVAMP	Zero-shot CoT	81.57	86.27	85.70	91.40	86.24
401		Few-shot CoT	<u>86.42</u>	91.73	94.50	<u>96.30</u>	<b>92.24</b>
402		SC@maj64	83.57	<u>88.37</u>	93.80	<u>95.60</u>	90.34
403		rStar	84.69	86.40	92.15	<u>95.90</u>	89.79
404		ToT	83.31	89.87	88.60	93.50	88.82
405		RAP	85.64	<u>91.90</u>	84.50	90.70	88.19
406		TS-LLM	83.25	89.82	93.92	94.24	90.81
407		PPO-MCTS	85.24	89.76	93.15	94.82	90.74
408		EcoNash	<b>87.79</b>	<b>92.27</b>	<b>96.80</b>	<b>97.20</b>	<b>93.52</b>
409	StrategyQA	Zero-shot CoT	55.13	67.91	75.21	78.56	69.20
410		Few-shot CoT	62.79	82.38	82.57	85.30	78.26
411		SC@maj64	65.45	81.27	79.33	82.07	77.03
412		rStar	68.64	<u>86.70</u>	83.45	87.86	<u>81.66</u>
413		ToT	<b>71.29</b>	84.49	80.15	84.17	80.03
414		RAP	69.38	82.27	83.29	87.92	80.72
415		TS-LLM	68.12	83.82	<u>84.24</u>	90.46	81.65
416		PPO-MCTS	67.85	82.94	83.76	89.24	80.95
417		EcoNash	<u>70.21</u>	<b>88.27</b>	<b>87.39</b>	<b>94.30</b>	<b>85.04</b>
418	MATH	Zero-shot CoT	25.17	54.17	68.24	73.82	55.35
419		Few-shot CoT	33.38	66.45	74.41	80.30	63.64
420		SC@maj64	31.58	62.21	67.39	78.25	59.86
421		rStar	<b>37.89</b>	<u>70.28</u>	71.57	83.49	65.81
422		ToT	34.35	65.22	60.41	82.88	60.72
423		RAP	33.99	62.53	68.71	80.23	61.37
424		TS-LLM	34.82	67.85	<u>76.92</u>	<u>83.76</u>	<b>65.84</b>
425		PPO-MCTS	34.76	65.82	73.45	81.24	63.82
426		EcoNash	<u>37.02</u>	<b>72.29</b>	<b>81.47</b>	<b>87.50</b>	<b>69.07</b>

StrategyQA datasets, aiming to address three key questions: (1) To what extent can weaker LLMs be enhanced? (examined on LLaMA 3.1 8B), (2) Can stronger LLMs be further improved? (using LLaMA 3.1 70B), and (3) Should the number of Coordinator LLMs be increased along with the number of Execution LLMs? Starting from three Execution LLMs (as in the main results), we gradually increased the number of agents to nine. We used the few-shot CoT as the baseline (in grey line) as Figure2. The results suggest that beyond four Execution LLMs, performance improvements were minimal, and in some cases, performance even declined. We attribute this to the challenge faced by the Coordinator LLM in managing an excessive number of Execution LLMs, making it difficult to achieve optimal coordination by redundant information from the additional agents.

Instead of simply increasing the number of Execution LLMs, we enhance scalability by forming a global Nash equilibrium through local Nash equilibria by introducing additional coordinators. This setup ensures that each Coordinator handles a reasonable amount of data. Specifically, each Coordinator manages up to 4 Execution LLMs, forming commitments and guiding them toward local Nash equilibria. Furthermore, a central LLM was introduced to coordinate the multiple coordinators, facilitating the transition from local Nash equilibria to a global Nash equilibrium (details in Appendix 2). We observed significant improvements across all benchmarks, both for weaker models(Llama 3.1 8B) and stronger models (Llama 3.1 70B). Compared to a system with 3

432 Table 2: Empirical results on the TravelPlanner dataset, along with some leaderboard rankings, are  
 433 presented. The best performance is highlighted in bold.

	Validation (#180)								Test (#1,000)							
	Delivery Rate	Commonsense Pass Rate		Hard Constraint Pass Rate		Final Pass Rate	Delivery Rate	Commonsense Pass Rate		Hard Constraint Pass Rate		Final Pass Rate				
		Micro	Macro	Micro	Macro			Micro	Macro	Micro	Macro					
Greedy Search	100	74.4	0	60.8	37.8	0	100	72.0	0	52.4	31.8	0				
Two-stage																
Mixtral-8x7B-MoE	49.4	30.0	0	1.2	0.6	0	51.2	32.2	0.2	0.7	0.4	0				
Gemini Pro	28.9	18.9	0	0.5	0.6	0	39.1	24.9	0	0.6	0.1	0				
GPT-3.5-Turbo	86.7	54.0	0	0	0	0	91.8	57.9	0	0.5	0.6	0				
GPT-4-Turbo	89.4	61.1	2.8	15.2	10.6	0.6	93.1	63.3	2.0	10.5	5.5	0.6				
Debate(GPT-4)@3round	95.2	67.3	6.7	22.7	13.1	2.3	97.8	72.4	11.3	17.4	12.1	3.7				
EcoNash(GPT-4)	<b>100</b>	<b>71.4</b>	<b>15.6</b>	<b>32.1</b>	<b>25.7</b>	<b>7.2</b>	<b>100</b>	<b>82.1</b>	<b>26.6</b>	<b>32.4</b>	<b>17.6</b>	<b>9.3</b>				
Sole-planning																
DirectGPT-3.5-Turbo	100	60.2	4.4	11.0	2.8	0	100	59.5	2.7	9.5	4.4	0.6				
CoT-GPT-3.5-Turbo	100	66.3	3.3	11.9	5.0	0	100	64.4	2.3	9.8	3.8	0.4				
ReActGPT-3.5-Turbo	82.2	47.6	3.9	11.4	6.7	0.6	81.6	45.9	2.5	10.7	3.1	0.7				
ReflexION(GPT-3.5-Turbo)	93.9	53.8	2.8	11.0	2.8	0	92.1	52.1	2.2	9.9	3.8	0.6				
DirectMixtral-8x7B-MoE	100	68.1	5.0	3.3	1.1	0	99.3	67.0	3.7	3.9	1.6	0.7				
DirectGemini Pro	93.9	65.0	8.3	9.3	4.4	0.6	93.7	64.7	7.9	10.6	4.7	2.1				
DirectGPT-4-Turbo	<b>100</b>	80.4	17.2	47.1	22.2	4.4	<b>100</b>	80.6	15.2	44.3	23.1	4.4				
Debate(GPT-4)	97.7	78.9	15.6	43.3	20.6	6.7	98.2	79.5	18.8	41.7	22.9	7.1				
EcoNash(GPT-4)	<b>100</b>	<b>83.3</b>	<b>22.2</b>	<b>51.7</b>	<b>27.8</b>	<b>12.9</b>	<b>100</b>	<b>84.2</b>	<b>23.5</b>	<b>49.8</b>	<b>28.7</b>	<b>15.2</b>				

Table 3: Performance of different configurations in Execution LLMs on GSM-Hard and MATH.

Method	GSM-Hard	MATH
<b>Baselines</b>		
EcoNash	51.43	81.47
LLaMA 3.1 70b (Few-shot CoT)	42.23	62.71
<b>EcoNash Configurations</b>		
Homog. (3x Llama3.1 8b)	48.71	67.70
Homog. (3x Llama3.1 405b)	61.29	89.24
Heterog. (Llama3.1 8b, Llama3 8b, Mixtral 7b)	45.24	74.24
Heterog. (Mixtral 8x22b, Qwen1.5 110b, Llama3.1 405b)	55.73	85.46

Execution LLMs and one coordinator, the scaled-up system with 9 Execution LLMs, 3 coordinators, and a central LLM achieved 18.1% improvement in Figure 3, which has potential to further scale up.

#### 4.5 ABLATION STUDY

In the additional experiments, heterogeneous Execution LLMs experienced a slight performance decline. An intuitive explanation for this observation is that implementing BNE is more challenging for heterogeneous Execution LLMs. To verify the actual performance differences of the EcoNash framework before and after achieving BNE, we conducted experiments on three math reasoning benchmarks: GSM8K, GSM-Hard, and MATH. Results in Table 5 demonstrate that our framework achieved an average performance improvement of 14% after implementing BNE.

Table 4: Average token usage and performance comparison in the Math, GSM8K, and GSM-Hard.

Dataset	Inference Strategy	LLaMA3.1 70B		Mixtral 8x7b		Mixtral 8x22b	
		Token Usage	Performance	Token Usage	Performance	Token Usage	Performance
Math	EcoNash	1629.79	81.47	1128.23	35.02	4270.86	72.29
	Multi-Agent Debate (3 rounds)	2154.87	71.58	1462.12	31.28	5345.56	67.41
	RAP	2653.27	68.71	1737.73	33.99	6668.55	62.53
	EcoNash (with detailed strategy)	3270.06	72.38	2150.23	26.18	8054.03	68.23
	Self Consistency (64 rounds)	11917.00	67.39	8066.21	31.58	29616.13	62.21
GSM8K	EcoNash	1131.65	92.70	1284.98	76.97	4715.31	88.20
	Multi-Agent Debate (3 rounds)	1391.57	86.32	1463.40	70.19	5714.05	81.95
	RAP	1907.86	81.33	1248.66	72.03	6517.77	76.97
	EcoNash (with detailed strategy)	2772.24	85.17	1188.13	65.37	9341.60	81.46
	Self Consistency (64 rounds)	9574.25	89.56	6601.34	71.08	24671.91	86.24
GSM-Hard	EcoNash	1518.76	51.43	1271.53	25.76	7101.62	47.58
	Multi-Agent Debate (3 rounds)	3030.73	41.98	1478.14	20.04	9250.78	45.21
	RAP	1768.72	38.97	1036.11	22.47	6464.52	42.79
	EcoNash (with detailed strategy)	3662.64	44.12	2239.07	18.52	11464.98	41.04
	Self Consistency (64 rounds)	16724.69	39.76	11668.19	22.47	74544.25	44.19

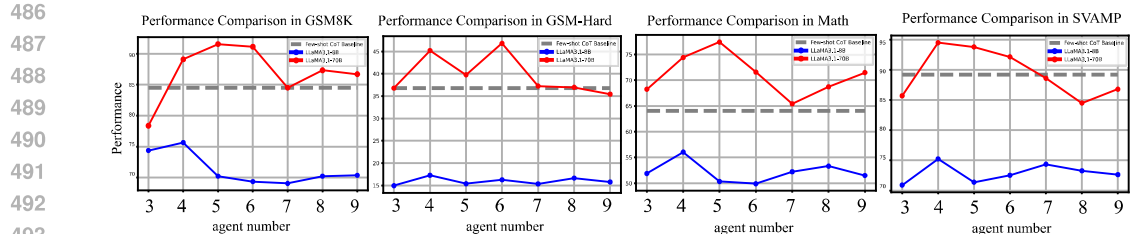


Figure 2: Scaling up our framework with a single coordinator while increasing the number of Execution LLMs. Experiments were conducted on GSM8K, GSM-Hard, Math, and SVAMP datasets.

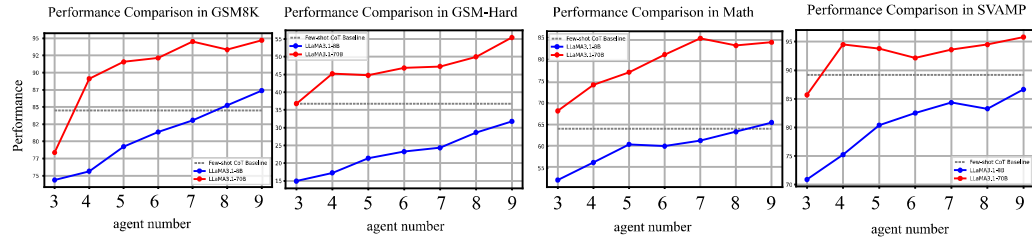


Figure 3: Scaling up our framework involves increasing the number of coordinators in proportion to the growing number of Execution LLMs, with coordinators scaling accordingly. Experiments were conducted on the GSM8K, GSM-Hard, MATH, and SVAMP datasets.

Table 5: Performance comparison of models with and without BNE across different datasets.

Dataset	Model	Without BNE (%)	With BNE (%)
GSM8K	LLaMA3.1-8B	74.38	80.33
	LLaMA3.1-70B	82.12	96.61
	LLaMA3.1-405B	92.36	100.00
GSM-Hard	LLaMA3.1-8B	21.73	30.71
	LLaMA3.1-70B	43.58	60.26
	LLaMA3.1-405B	51.54	65.91
MATH	LLaMA3.1-8B	55.92	71.45
	LLaMA3.1-70B	74.47	87.31
	LLaMA3.1-405B	82.31	94.78

Table 6: Ablation on reward.

	$R_1$	$R_2$	$R_3$	EcoNash
✓	✗	✓		77.55
✓	✗	✗		74.32
✓	✓	✗		76.21
Random				62.71

Table 7: Ablation on strategy.

	$S_1$	$S_2$	$S_3$	EcoNash
✓	✗	✗		71.35
✗	✓	✗		72.31
✗	✗	✓		81.47

Additionally, we performed ablation studies on various submodules, including the reward design and the setting where the Coordinator LLM provides a strategy without giving a direct answer, to ensure the validity of our architecture. All experiments were conducted with Llama 3.1-70B model, tested on the MATH benchmark. Specifically,  $R_1$  refers to the action likelihood reward,  $R_2$  to the task-specific reward, and  $R_3$  to the self-evaluation reward.  $S_1$  represents the setting where the coordinator does not provide any strategy, while  $S_2$  represents the setting where the coordinator provides both a detail strategy,  $S_3$  represents EcoNash, with informative strategy as our baseline.

## 5 CONCLUSION

In this work, we introduce EcoNash, a novel collaborative reasoning framework in multi-LLM systems. EcoNash constructs a hierarchical coordination mechanism, enabling multiple Execution LLMs to engage in distributed reasoning guided by a Coordinator LLM. The hierarchical coordination mechanism allows each Execution LLM to operate independently with its own belief network, receiving only the question and strategy from the Coordinator LLM. This enables multiple Execution LLMs to engage in distributed reasoning, guided by the Coordinator LLM, to achieve BNE. Experimental results across six benchmarks demonstrate EcoNash outperforms single-agent approaches by 10.9% and surpasses the performance of existing multi-agent methods by 11.2% in average, confirming the robustness and efficiency of our framework. Moreover, EcoNash demonstrate great potential to scale up the mulit-LLMs system while maintain relatively reasonable consumption cost.

540  
541 ETHIC STATEMENT

542 The study does not involve human subjects, data set releases, potentially harmful insights, applica-  
 543 tions, conflicts of interest, sponsorship, discrimination, bias, fairness concerns, privacy or security  
 544 issues, legal compliance issues, or research integrity issues.

545  
546 REPRODUCIBILITY STATEMENT  
547

548 The experimental setups for training and evaluation are described in detail in Section 4.1, and the  
 549 experiments are all conducted using public datasets. We provide the link to our source codes to en-  
 550 sure the reproducibility of our experimental results: [https://anonymous.4open.science/](https://anonymous.4open.science/status/EcoNash-867A)  
 551 status/EcoNash-867A.

552  
553 REFERENCES  
554

555 Jamshaid Ahmad, Abdullah Eqal Al-Mazrooei, and Themistocles M Rassias. Common fixed point  
 556 theorems with applications to theoretical computer science. *International Journal of Nonlinear*  
 557 *Analysis and Applications*, 14(2):1–10, 2023.

558 Vivek S Borkar. *Stochastic Approximation: A Dynamical Systems Viewpoint*. Cambridge University  
 559 Press, Cambridge, UK, 2009.

560 Tom Brown, Benjamin Mann, Nick Ryder, Melanie Subbiah, Jared D Kaplan, Prafulla Dhariwal,  
 561 Aryind Neelakantan, Pranav Shyam, Girish Sastry, Amanda Askell, et al. Language models are  
 562 few-shot learners. In *NeurIPS*, 2020.

563 Chi-Min Chan, Weize Chen, Yusheng Su, Jianxuan Yu, Wei Xue, Shanghang Zhang, Jie Fu, and  
 564 Zhiyuan Liu. Chateval: Towards better llm-based evaluators through multi-agent debate. In  
 565 *ICLR*, 2024.

566 Justin Chih-Yao Chen, Swarnadeep Saha, and Mohit Bansal. Reconcile: Round-table conference  
 567 improves reasoning via consensus among diverse llms. *arXiv preprint arXiv:2309.13007*, 2023.

568 Yew Ken Chia, Guizhen Chen, Luu Anh Tuan, Soujanya Poria, and Lidong Bing. Contrastive chain-  
 569 of-thought prompting. *arXiv preprint arXiv:2311.09277*, 2023.

570 Karl Cobbe, Vineet Kosaraju, Mohammad Bavarian, Mark Chen, Heewoo Jun, Lukasz Kaiser,  
 571 Matthias Plappert, Jerry Tworek, Jacob Hilton, Reiichiro Nakano, et al. Training verifiers to  
 572 solve math word problems. *arXiv preprint arXiv:2110.14168*, 2021.

573 Yilun Du, Shuang Li, Antonio Torralba, Joshua B Tenenbaum, and Igor Mordatch. Improving  
 574 factuality and reasoning in language models through multiagent debate. In *ICML*, 2024.

575 Abhimanyu Dubey, Abhinav Jauhri, Abhinav Pandey, Abhishek Kadian, Ahmad Al-Dahle, Aiesha  
 576 Letman, Akhil Mathur, Alan Schelten, Amy Yang, Angela Fan, et al. The llama 3 herd of models.  
 577 *arXiv preprint arXiv:2407.21783*, 2024.

578 Xidong Feng, Ziyu Wan, Muning Wen, Stephen Marcus McAleer, Ying Wen, Weinan Zhang, and  
 579 Jun Wang. Alphazero-like tree-search can guide large language model decoding and training.  
 580 *arXiv preprint arXiv:2309.17179*, 2023.

581 Jakob Foerster, Richard Y Chen, Maruan Al-Shedivat, Shimon Whiteson, Pieter Abbeel, and Igor  
 582 Mordatch. Learning to model other minds: A deep learning framework for social intelligence. In  
 583 *Proceedings of the 32nd Conference on Neural Information Processing Systems*, pp. 8112–8122,  
 584 2018a.

585 Jakob Foerster, Gregory Farquhar, Triantafyllos Afouras, Nantas Nardelli, and Shimon Whiteson.  
 586 Counterfactual multi-agent policy gradients. In *Proceedings of the AAAI conference on artificial*  
 587 *intelligence*, volume 32, 2018b.

588 Yao Fu, Hao Peng, Ashish Sabharwal, Peter Clark, and Tushar Khot. Complexity-based prompting  
 589 for multi-step reasoning. *arXiv preprint arXiv:2210.00720*, 2022.

- 594 Drew Fudenberg and David K Levine. *The Theory of Learning in Games*. MIT Press, Cambridge,  
 595 MA, 1998.
- 596
- 597 Scott Fujimoto, Herke Hoof, and David Meger. Addressing function approximation error in actor-  
 598 critic methods. In *International conference on machine learning*, pp. 1587–1596. PMLR, 2018.
- 599
- 600 Luyu Gao, Aman Madaan, Shuyan Zhou, Uri Alon, Pengfei Liu, Yiming Yang, Jamie Callan, and  
 601 Graham Neubig. Pal: Program-aided language models. In *ICML*, 2023.
- 602
- 603 Mor Geva, Daniel Khashabi, Elad Segal, Tushar Khot, Dan Roth, and Jonathan Berant. Did aristotle  
 604 use a laptop? a question answering benchmark with implicit reasoning strategies. *Transactions of  
 605 the Association for Computational Linguistics*, 9:346–361, 2021.
- 606
- 607 Shibo Hao, Yi Gu, Haodi Ma, Joshua Jiahua Hong, Zhen Wang, Daisy Zhe Wang, and Zhiting Hu.  
 608 Reasoning with language model is planning with world model. *arXiv preprint arXiv:2305.14992*,  
 609 2023.
- 610 Elad Hazan. *Introduction to Online Convex Optimization*. Now Publishers Inc, Boston, MA, 2016.
- 611
- 612 Dan Hendrycks, Collin Burns, Saurav Kadavath, Akul Arora, Steven Basart, Eric Tang, Dawn Song,  
 613 and Jacob Steinhardt. Measuring mathematical problem solving with the math dataset. *arXiv  
 614 preprint arXiv:2103.03874*, 2021.
- 615
- 616 Sirui Hong, Xiawu Zheng, Jonathan Chen, Yuheng Cheng, Jinlin Wang, Ceyao Zhang, Zili Wang,  
 617 Steven Ka Shing Yau, Zijuan Lin, Liyang Zhou, et al. Metagpt: Meta programming for multi-  
 618 agent collaborative framework. *arXiv preprint arXiv:2308.00352*, 2023.
- 619
- 620 Natasha Jaques, Angeliki Lazaridou, Edward Hughes, Caglar Gulcehre, Pedro A Ortega, DJ Strouse,  
 621 Joel Z Leibo, and Nando De Freitas. Social influence as intrinsic motivation for multi-agent  
 622 deep reinforcement learning. In *Proceedings of the 36th International Conference on Machine  
 623 Learning*, pp. 3040–3049, 2019.
- 624
- 625 Albert Q Jiang, Alexandre Sablayrolles, Arthur Mensch, Chris Bamford, Devendra Singh Chaplot,  
 626 Diego de las Casas, Florian Bressand, Gianna Lengyel, Guillaume Lample, Lucile Saulnier, et al.  
 627 Mistral 7b. *arXiv preprint arXiv:2310.06825*, 2023.
- 628
- 629 Chi Jin, Zhuoran Yang, Zhaoran Wang, and Michael I Jordan. Provably efficient reinforcement  
 630 learning with linear function approximation. In *Conference on learning theory*, pp. 2137–2143.  
 631 PMLR, 2020.
- 632
- 633 Takeshi Kojima, Shixiang Shane Gu, Machel Reid, Yutaka Matsuo, and Yusuke Iwasawa. Large  
 634 language models are zero-shot reasoners. In *NeurIPS*, 2022.
- 635
- 636 Landon Kraemer and Bikramjit Banerjee. Multi-agent reinforcement learning as a rehearsal for  
 637 decentralized planning. *Neurocomputing*, 190:82–94, 2016.
- 638
- 639 Xiaochong Lan, Chen Gao, Depeng Jin, and Yong Li. Stance detection with collaborative role-  
 640 infused llm-based agents. In *Proceedings of the International AAAI Conference on Web and  
 641 Social Media*, volume 18, pp. 891–903, 2024.
- 642
- 643 Marc Lanctot, Vinicius Zambaldi, Audrunas Gruslys, Angeliki Lazaridou, Karl Tuyls, Julien  
 644 Pérolat, David Silver, and Thore Graepel. A unified game-theoretic approach to multiagent re-  
 645 enforcement learning. In *Advances in Neural Information Processing Systems*, pp. 4190–4203,  
 646 2017.
- 647
- Tian Liang, Zhiwei He, Wenxiang Jiao, Xing Wang, Yan Wang, Rui Wang, Yujiu Yang, Zhaopeng  
 Tu, and Shuming Shi. Encouraging divergent thinking in large language models through multi-  
 agent debate. *arXiv preprint arXiv:2305.19118*, 2023.
- Jiacheng Liu, Andrew Cohen, Ramakanth Pasunuru, Yejin Choi, Hannaneh Hajishirzi, and Asli  
 Celikyilmaz. Don’t throw away your value model! generating more preferable text with value-  
 guided monte-carlo tree search decoding. In *First Conference on Language Modeling*, 2024.

- 648 Jie Liu, Zhiwei Ding, Yong Liu, and Xinwei Wang. Decentralized multi-agent reinforcement learning  
 649 with networked agents: Recent advances. *Foundations and Trends in Machine Learning*, 15  
 650 (1):1–120, 2022.
- 651 Li-Chun Lu, Shou-Jen Chen, Tsung-Min Pai, Chan-Hung Yu, Hung-yi Lee, and Shao-Hua Sun.  
 652 Ilm discussion: Enhancing the creativity of large language models via discussion framework and  
 653 role-play. *arXiv preprint arXiv:2405.06373*, 2024.
- 654 Arkadi Nemirovski, Anatoli Juditsky, Guanghui Lan, and Alexander Shapiro. Robust stochastic  
 655 approximation approach to stochastic programming. *SIAM Journal on Optimization*, 19(4):1574–  
 656 1609, 2009.
- 657 Martin Owe and Christopher A Sims. Information theoretic limits of strategic communication.  
 658 *Journal of Economic Theory*, 148(6):2404–2434, 2013.
- 659 Arkil Patel, Satwik Bhattacharya, and Navin Goyal. Are nlp models really able to solve simple math  
 660 word problems? *arXiv preprint arXiv:2103.07191*, 2021.
- 661 Chau Pham, Boyi Liu, Yingxiang Yang, Zhengyu Chen, Tianyi Liu, Jianbo Yuan, Bryan A Plummer,  
 662 Zhaoran Wang, and Hongxia Yang. Let models speak ciphers: Multiagent debate through  
 663 embeddings. *arXiv preprint arXiv:2310.06272*, 2023.
- 664 Zhenting Qi, Mingyuan Ma, Jiahang Xu, Li Lyra Zhang, Fan Yang, and Mao Yang. Mutual reasoning  
 665 makes smaller llms stronger problem-solvers. *arXiv preprint arXiv:2408.06195*, 2024.
- 666 Shai Shalev-Shwartz. *Online Learning and Online Convex Optimization*. Now Publishers Inc,  
 667 Boston, MA, 2012.
- 668 Andries Petrus Smit, Nathan Grinsztajn, Paul Duckworth, Thomas D Barrett, and Arnu Pretorius.  
 669 Should we be going mad? a look at multi-agent debate strategies for llms. In *ICML*, 2024.
- 670 Richard S Sutton and Andrew G Barto. *Reinforcement Learning: An Introduction*. MIT Press,  
 671 Cambridge, MA, 2 edition, 2018.
- 672 Xingchen Wan, Ruoxi Sun, Hanjun Dai, Sercan O Arik, and Tomas Pfister. Better zero-shot reasoning  
 673 with self-adaptive prompting. *arXiv preprint arXiv:2305.14106*, 2023.
- 674 Xuezhi Wang, Jason Wei, Dale Schuurmans, Quoc Le, Ed Chi, Sharan Narang, Aakanksha Chowdhury,  
 675 and Denny Zhou. Self-consistency improves chain of thought reasoning in language models.  
 676 In *ICLR*, 2023.
- 677 Jason Wei, Xuezhi Wang, Dale Schuurmans, Maarten Bosma, Fei Xia, Ed Chi, Quoc V Le, Denny  
 678 Zhou, et al. Chain-of-thought prompting elicits reasoning in large language models. In *NeurIPS*,  
 679 2022.
- 680 Qingyun Wu, Gagan Bansal, Jieyu Zhang, Yiran Wu, Beibin Li, Erkang Zhu, Li Jiang, Xiaoyun  
 681 Zhang, Shaokun Zhang, Jiale Liu, et al. Autogen: Enabling next-gen llm applications via multi-  
 682 agent conversation. In *ICLR 2024 Workshop on Large Language Model (LLM) Agents*, 2024.
- 683 Zhaofeng Wu, Linlu Qiu, Alexis Ross, Ekin Akyürek, Boyuan Chen, Bailin Wang, Najoung Kim,  
 684 Jacob Andreas, and Yoon Kim. Reasoning or reciting? exploring the capabilities and limitations  
 685 of language models through counterfactual tasks. *arXiv preprint arXiv:2307.02477*, 2023.
- 686 Jian Xie, Kai Zhang, Jiangjie Chen, Tinghui Zhu, Renze Lou, Yuandong Tian, Yanghua Xiao, and  
 687 Yu Su. Travelplanner: A benchmark for real-world planning with language agents. *arXiv preprint  
 688 arXiv:2402.01622*, 2024a.
- 689 Yuxi Xie, Kenji Kawaguchi, Yiran Zhao, James Xu Zhao, Min-Yen Kan, Junxian He, and Michael  
 690 Xie. Self-evaluation guided beam search for reasoning. *Advances in Neural Information Processing  
 691 Systems*, 36, 2024b.
- 692 Shunyu Yao, Jeffrey Zhao, Dian Yu, Nan Du, Izhak Shafran, Karthik Narasimhan, and Yuan Cao.  
 693 React: Synergizing reasoning and acting in language models. *arXiv preprint arXiv:2210.03629*,  
 694 2022.

- 702 Shunyu Yao, Dian Yu, Jeffrey Zhao, Izhak Shafran, Tom Griffiths, Yuan Cao, and Karthik  
703 Narasimhan. Tree of thoughts: Deliberate problem solving with large language models. In  
704 *NeurIPS*, 2023.
- 705 Zhangyue Yin, Qiushi Sun, Cheng Chang, Qipeng Guo, Junqi Dai, Xuan-Jing Huang, and Xipeng  
706 Qiu. Exchange-of-thought: Enhancing large language model capabilities through cross-model  
707 communication. In *Proceedings of the 2023 Conference on Empirical Methods in Natural Lan-*  
708 *guage Processing*, pp. 15135–15153, 2023.
- 709 Siyu Yuan, Kaitao Song, Jiangjie Chen, Xu Tan, Dongsheng Li, and Deqing Yang. Evo-  
710 agent: Towards automatic multi-agent generation via evolutionary algorithms. *arXiv preprint arXiv:2406.14228*, 2024a.
- 711 Weizhe Yuan, Ilia Kulikov, Ping Yu, Kyunghyun Cho, Sainbayar Sukhbaatar, Jason Weston, and  
712 Jing Xu. Following length constraints in instructions. *arXiv preprint arXiv:2406.17744*, 2024b.
- 713 Jintian Zhang, Xin Xu, and Shumin Deng. Exploring collaboration mechanisms for llm agents: A  
714 social psychology view. *arXiv preprint arXiv:2310.02124*, 2023a.
- 715 Kaiqing Zhang, Zhuoran Yang, and Tamer Başar. Multi-agent deep reinforcement learning: A  
716 survey. *IEEE Transactions on Artificial Intelligence*, 2(6):503–527, 2021.
- 717 Zhihuosheng Zhang, Aston Zhang, Mu Li, and Alex Smola. Automatic chain of thought prompting in  
718 large language models. In *ICLR*, 2023b.
- 719 Lianmin Zheng, Wei-Lin Chiang, Ying Sheng, Siyuan Zhuang, Zhanghao Wu, Yonghao Zhuang,  
720 Zi Lin, Zhiuhuan Li, Dacheng Li, Eric Xing, et al. Judging llm-as-a-judge with mt-bench and  
721 chatbot arena. *Advances in Neural Information Processing Systems*, 36:46595–46623, 2023.
- 722 Denny Zhou, Nathanael Schärli, Le Hou, Jason Wei, Nathan Scales, Xuezhi Wang, Dale Schuur-  
723 mans, Claire Cui, Olivier Bousquet, Quoc Le, et al. Least-to-most prompting enables complex  
724 reasoning in large language models. *arXiv preprint arXiv:2205.10625*, 2022.
- 725 Banghua Zhu, Michael Jordan, and Jiantao Jiao. Principled reinforcement learning with human feed-  
726 back from pairwise or k-wise comparisons. In *International Conference on Machine Learning*,  
727 pp. 43037–43067. PMLR, 2023.
- 728
- 729
- 730
- 731
- 732
- 733
- 734
- 735
- 736
- 737
- 738
- 739
- 740
- 741
- 742
- 743
- 744
- 745
- 746
- 747
- 748
- 749
- 750
- 751
- 752
- 753
- 754
- 755

756 A THEORETICAL PROOF  
757758 A.1 PROOF OF THEOREM 1  
759

760 *Proof.* We aim to prove the existence of a Bayesian Nash Equilibrium (BNE) in our multi-agent  
761 LLM framework under the specified conditions. The proof proceeds by verifying the conditions of  
762 Glicksberg’s Fixed Point Theorem, which guarantees the existence of a fixed point in continuous  
763 games with infinite-dimensional strategy spaces.

764 **Step 1: Define the Best Response Correspondence**  
765

766 For each agent  $i$ , define the best response correspondence  $BR_i$  as:

$$767 BR_i(\pi_{-i}) = \{\pi_i \in \Pi_i \mid \pi_i \text{ maximizes } U_i(\theta_i, \pi_i, \pi_{-i})\},$$

768 where  $\Pi_i$  is the set of all admissible strategies for agent  $i$ , and  $\pi_{-i}$  denotes the strategies of all other  
769 agents.  
770

771 **Step 2: Verify the Conditions of Glicksberg’s Fixed Point Theorem**  
772

773 To apply Glicksberg’s Fixed Point Theorem, we need to verify the following conditions for each  
774 agent  $i$ :

775 1. *Strategy Space Compactness and Convexity:*  
776

- 777 • The strategy space  $\Pi_i$  is non-empty, convex, and compact in the topology of pointwise  
778 convergence.

779 2. *Continuity of Payoff Functions:*  
780

- 781 • The payoff function  $U_i(\theta_i, \pi_i, \pi_{-i})$  is continuous in  $(\pi_i, \pi_{-i})$  for each fixed  $\theta_i$ .

782 3. *Quasi-Concavity of Payoff Functions:*  
783

- 784 • The payoff function  $U_i(\theta_i, \pi_i, \pi_{-i})$  is quasi-concave in  $\pi_i$  for each fixed  $\theta_i$  and  $\pi_{-i}$ .  
785

786 *Verification:*

787 1. **Strategy Space Compactness and Convexity:**  
788

789 The strategy space  $\Pi_i$  consists of all measurable functions mapping types  $\theta_i$  to actions  $a_i$   
790 in  $\mathcal{A}_i$ . Since  $\Theta_i$  and  $\mathcal{A}_i$  are compact metric spaces, and strategies are measurable functions  
791 from one compact space to another, the space of such functions  $\Pi_i$  can be endowed with  
792 the topology of pointwise convergence, making it compact by Tychonoff’s Theorem. Convexity  
793 follows because the set of mixed (probabilistic) strategies is convex, and any convex  
794 combination of measurable functions is measurable.

795 2. **Continuity of Payoff Functions:**  
796

797 For fixed  $\theta_i$ , the payoff function  $U_i(\theta_i, \pi_i, \pi_{-i})$  depends continuously on  $\pi_i$  and  $\pi_{-i}$  due  
798 to the continuity of  $U_i$  in actions and types. Specifically, since  $U_i$  is continuous in  $a =$   
799  $(a_i, a_{-i})$  and the strategies  $\pi_i, \pi_{-i}$  map continuously from types to actions, the composition  
800  $U_i(\theta_i, \pi_i(\theta_i), \pi_{-i}(\theta_{-i}))$  is continuous in  $(\pi_i, \pi_{-i})$ .

801 3. **Quasi-Concavity of Payoff Functions:**  
802

803 For each  $\theta_i$  and  $\pi_{-i}$ , the function  $\pi_i \mapsto U_i(\theta_i, \pi_i, \pi_{-i})$  is quasi-concave because  $U_i$  is  
804 quasi-concave in  $a_i$  and the strategies are linear in the space of mixed strategies. There-  
805 fore, any convex combination of strategies does not decrease the utility, satisfying quasi-  
806 concavity.

807 **Step 3: Establish Upper Hemicontinuity and Non-Empty, Convex-Valuedness of Best Re-  
808 sponse Correspondences**  
809

We need to show that  $BR_i(\pi_{-i})$  is upper hemicontinuous with non-empty, convex values.

- 810     1. **Non-Empty, Convex Values:**  
 811  
 812     For each  $\pi_{-i}$ , since  $\Pi_i$  is compact and convex, and  $U_i$  is continuous and quasi-concave in  
 813      $\pi_i$ , the Weierstrass Theorem ensures that the maximum exists; hence,  $BR_i(\pi_{-i})$  is non-  
 814     empty. Convexity follows from the quasi-concavity of  $U_i$  in  $\pi_i$ , implying that any convex  
 815     combination of best responses is also a best response.  
 816     2. **Upper Hemicontinuity:**  
 817  
 818     Upper hemicontinuity of  $BR_i$  means that for any net  $\pi_{-i}^\alpha \rightarrow \pi_{-i}$ , and any  $\pi_i \in BR_i(\pi_{-i})$ ,  
 819     there exists a net  $\pi_i^\alpha \in BR_i(\pi_{-i}^\alpha)$  such that  $\pi_i^\alpha \rightarrow \pi_i$ . This property holds because the  
 820     payoff function  $U_i$  is continuous in  $(\pi_i, \pi_{-i})$ , and the strategy spaces are compact.

821     **Step 4: Application of Glicksberg's Fixed Point Theorem**

823     Having verified all the conditions, we can apply Glicksberg's Fixed Point Theorem, which states  
 824     that if each player's strategy set is compact and convex, and their payoff functions are continuous  
 825     and quasi-concave in their own strategies, then the game has at least one Nash Equilibrium in mixed  
 826     strategies.

827     **Step 5: Conclusion**

829     Therefore, there exists a strategy profile  $\bar{\pi}^* = (\pi_1^*, \pi_2^*, \dots, \pi_N^*)$  such that for each agent  $i$ ,

$$\pi_i^* \in BR_i(\pi_{-i}^*),$$

832     meaning that no agent can unilaterally deviate to improve their expected payoff, given their beliefs  
 833     about other agents' types and strategies. This strategy profile constitutes a Bayesian Nash Equilib-  
 834     rium in our multi-agent LLM framework.

□

837     **A.2 PROOF OF PROPOSITION 1**

839     *Proof.* We aim to show that, by minimizing the TD loss for each agent's Q-network, the agents'  
 840     strategies converge to a Bayesian Nash Equilibrium (BNE).

841     **Assumptions:**

- 843  
 844     1. The Q-networks  $Q_i(\mathbf{s}, a_i; \theta_i)$  are parameterized by prompt embeddings  $\theta_i$ , and the mapping  
 845     from  $\theta_i$  to  $Q_i$  is continuously differentiable.  
 846     2. The exploration strategy ensures sufficient coverage of the state-action space (e.g.,  $\epsilon$ -greedy  
 847     with decaying  $\epsilon$ ).  
 848     3. The loss function  $L_i(\theta_i)$  is convex or has Lipschitz continuous gradients with respect to  $\theta_i$ .  
 849     4. The gradient  $\nabla_{\theta_i} L_i(\theta_i)$  is Lipschitz continuous.  
 850     5. The learning rate  $\eta_t$  is chosen such that it satisfies the Robbins-Monro conditions:  
 851      $\sum_{t=1}^{\infty} \eta_t = \infty$  and  $\sum_{t=1}^{\infty} \eta_t^2 < \infty$ .

855     **Step 1: Defining the TD Loss Function** The TD loss function for agent  $i$  is:

$$857 \quad L_i(\theta_i) = \mathbb{E}_{(\mathbf{s}, a_i, r_i, \mathbf{s}') \sim \mathcal{D}_i} \left[ \left( r_i + \gamma \max_{a'_i} Q_i(\mathbf{s}', a'_i; \theta_i^-) - Q_i(\mathbf{s}, a_i; \theta_i) \right)^2 \right]$$

860     This loss measures the discrepancy between the predicted Q-value and the target Q-value based on  
 861     the reward and the estimated optimal future Q-value.

862     **Step 2: Gradient Descent Update** Agent  $i$  updates its Q-network parameters according to:

$$863 \quad \theta_i^{t+1} = \theta_i^t - \eta_t \cdot \nabla_{\theta_i} L_i(\theta_i^t).$$

864 The gradient of the loss function with respect to the parameters is:  
 865

$$866 \nabla_{\theta_i} L_i(\theta_i^t) = \mathbb{E}_{(\mathbf{s}, a_i, r_i, \mathbf{s}') \sim \mathcal{D}_i} \left[ 2 \left( r_i + \gamma \max_{a'_i} Q_i(\mathbf{s}', a'_i; \theta_i^-) - Q_i(\mathbf{s}, a_i; \theta_i^t) \right) \cdot (-\nabla_{\theta_i} Q_i(\mathbf{s}, a_i; \theta_i^t)) \right]. \\ 867$$

869 **Step 3: Convergence of Gradient Descent with TD Loss** Under the assumptions that  $L_i(\theta_i)$   
 870 has Lipschitz continuous gradients and the learning rate  $\eta_t$  satisfies the Robbins-Monro conditions,  
 871 stochastic gradient descent converges to a stationary point  $\theta_i^*$  of  $L_i(\theta_i)$ :

$$872 \lim_{t \rightarrow \infty} \theta_i^t = \theta_i^*. \\ 873$$

874 At convergence, the gradient vanishes:  
 875

$$876 \nabla_{\theta_i} L_i(\theta_i^*) = 0,$$

877 which implies:  
 878

$$879 \mathbb{E}_{(\mathbf{s}, a_i, r_i, \mathbf{s}') \sim \mathcal{D}_i} \left[ \left( r_i + \gamma \max_{a'_i} Q_i(\mathbf{s}', a'_i; \theta_i^-) - Q_i(\mathbf{s}, a_i; \theta_i^*) \right) \cdot \nabla_{\theta_i} Q_i(\mathbf{s}, a_i; \theta_i^*) \right] = 0. \\ 880$$

881 Assuming that the Q-network parameterization is such that the above condition holds only when:  
 882

$$883 Q_i(\mathbf{s}, a_i; \theta_i^*) = r_i + \gamma \max_{a'_i} Q_i(\mathbf{s}', a'_i; \theta_i^-), \\ 884$$

885 the Q-network accurately estimates the expected cumulative rewards, aligning the agent's policy  
 886 with the optimal response to other agents' strategies.

887 **Step 4: Characterizing the Stationary Point** At the stationary point  $\theta_i^*$ , the Q-network satisfies  
 888 the Bellman optimality condition:  
 889

$$890 Q_i(\mathbf{s}, a_i; \theta_i^*) = r_i + \gamma \max_{a'_i} Q_i(\mathbf{s}', a'_i; \theta_i^-). \\ 891$$

892 This condition ensures that the agent's policy  $\pi_i(a_i | \mathbf{s}; \theta_i^*)$  is a best response to the current policies  
 893 of other agents, as it maximizes the expected cumulative reward.

894 **Step 5: Establishing Bayesian Nash Equilibrium** Since each agent's policy is a best response to  
 895 the policies of others, the set of policies  $\{\pi_i^*\}$  constitutes a Bayesian Nash Equilibrium. Each agent  
 896 maximizes its expected utility given its beliefs about other agents' types and strategies, fulfilling the  
 897 definition of BNE.  
 898 □

### 900 A.3 ASSUMPTIONS

902 Our theoretical analysis relies on four key assumptions that are both common in multi-agent systems  
 903 Zhang et al. (2021); Liu et al. (2022) and specifically relevant to our MA-LLM framework.

905 **Definition 1** (System Components). *In our MA-LLM framework:*

- 906 • *Each agent i's observation  $O_i = [e_t, e_s, \mathbf{b}_i]^\top$ , where  $e_t$  encodes the task,  $e_s$  represents the  
 907 coordinator's strategy, and  $\mathbf{b}_i$  is the belief state*
- 909 • *Each agent's action is its prompt embedding  $\mathbf{e}_i$  generated by belief network  $B_i(\tau_i, O_i; \theta_i^B)$*
- 911 • *The coordinator aggregates beliefs through  $f_e(\{\mathbf{b}_i\}_{i=1}^N; \theta_e)$  into group information  $\mathbf{E}$*

912 **Assumption 1** (Bounded Rewards). *The rewards from coordinator commitment are uniformly  
 913 bounded:  $|r_i(O_i, \mathbf{e}_i, \mathbf{E})| \leq R_{\max}$ , for all  $O_i, \mathbf{e}_i, \mathbf{E}, i$ .*

914 This assumption is standard in reinforcement learning Sutton & Barto (2018) and critical since it  
 915 ensures numerical stability in the learning process of LLMs, preventing reward explosion that could  
 916 lead to unstable training.

917 **Definition 2** (Historical Data and Posterior). *Given historical data  $D_t = \{(O_i^k, \mathbf{e}_i^k, C^k)\}_{k=1}^t$ :*

- 918     •  $P_{post}(\mathbf{E} | D_t, O_i, \mathbf{e}_i)$  is the posterior distribution over group information determined by the  
 919       coordinator  
 920  
 921     •  $P_{LLM}(\mathbf{E} | D_t, O_i, \mathbf{e}_i)$  is the belief distribution maintained by each execution LLM

922 **Assumption 2** (Approximate Posterior Alignment). Execution LLMs aim to align with the posterior  
 923 distributions determined by the Coordinator LLM within an acceptable error margin  $\epsilon > 0$ :

$$924 \quad 925 \quad D_{KL}(P_{LLM}(\mathbf{E} | D_t, O_i, \mathbf{e}_i) \| P_{post}(\mathbf{E} | D_t, O_i, \mathbf{e}_i)) \leq \epsilon,$$

926 where  $D_{KL}$  denotes the Kullback-Leibler divergence.

928 This approximate alignment acknowledges that perfect alignment is impractical but strives for a  
 929 close approximation:

- 930     • The Coordinator LLM acts as a centralized distributor of strategic guidance.  
 931  
 932     • Execution LLMs maintain belief alignment through prompt (detailed in Section 3.3.2).  
 933  
 934     • Monotonic guarantee in EcoNash mixing optimization network A.5.  
 935  
 936     • Such alignment has been shown in Foerster et al. (2018a); Jaques et al. (2019) to enhance  
 937 coordination.

938 **Definition 3** (Belief Entropy). For a given time  $t$ , the belief entropy  $H_t$  is defined as the Shannon  
 939 entropy of the aggregated belief embeddings:

$$939 \quad 940 \quad H_t = - \sum_{i=1}^N \mathbb{E}_{\mathbf{b}_i \sim B_i} [\mathbf{b}_i \log \mathbf{b}_i]$$

942 where  $B_i$  represents the belief network of agent  $i$ .

943 **Assumption 3** (Game Regularity). There exists  $\eta > 0$  such that for any  $t_1 < t_2$ , if  $H_{t_1} - H_{t_2} \leq$   
 944  $\log 2$ , then

$$945 \quad I(\theta_i^B; \xi(\mathbf{e}_i, \mathbf{E}) | D_{t_1}) \leq 4\eta \cdot I(\theta_i^B; \xi(\mathbf{e}_i, \mathbf{E}) | D_{t_2}),$$

946 for all agents  $i$ , where  $\theta_i^B$  are the belief network parameters.

947 This information-theoretic assumption serves multiple purposes in our framework:

- 948     • It ensures the stability of belief updates between LLMs over time by bounding the entropy  
 949       difference of belief states.  
 950  
 951     • The mutual information term  $I(\theta_i^B; \xi(\mathbf{e}_i, \mathbf{E}))$  quantifies how much an LLM's belief net-  
 952       work parameters affect its coordination through prompt embeddings.  
 953  
 954     • The bound  $4\eta$  controls the rate at which LLMs can adapt their belief states based on ob-  
 955       served interactions and coordinator guidance.

956 **Definition 4** (Value Function and Bellman Operator). For each execution LLM  $i$ :

- 957     • The value function  $V_t(O_i) = \mathbb{E}[\sum_{k=0}^{\infty} \gamma^k r_{t+k} | O_i^t = O_i]$  estimates the expected cumulative  
 958       rewards  
 959  
 960     • The optimal prompt embeddings  $\mathbf{e}_i^{*t}$  maximize the  $Q$ -function  $Q_i(O_i, \mathbf{e}_i; \theta_i^B)$  at time  $t$   
 961  
 962     • The Bellman operator  $B_t$  transforms one value function to another:  $(B_t V)(O_i) =$   
 963        $\max_{\mathbf{e}_i} \mathbb{E}[r_i + \gamma V(O_i') | O_i, \mathbf{e}_i]$

964 **Assumption 4** (Concentrability). There exists  $\kappa < \infty$  such that

$$965 \quad 966 \quad \mathbb{E} \left[ \sum_{t=1}^T \sum_{i=1}^N ((B_t - B^*)V_t)^2 (O_i^t, \mathbf{e}_i^{*t}, \mathbf{E}^{*t}) \right] \leq \kappa^2 T,$$

967 where  $B^*$  is the true Bellman operator.

968 This assumption is fundamental to our theoretical guarantees:

- It ensures that the value function estimates by each LLM converge to their true values at an appropriate rate.
  - The constant  $\kappa$  bounds the cumulative estimation error across all LLMs, critical for establishing our regret bounds.
  - In our MA-LLM system, this translates to the stability of response quality improvements during training.

**Collective Impact:** Together, these assumptions enable us to:

- Establish the existence of BNE in our MA-LLM system (Theorem 1)
  - Derive meaningful regret bounds for the learning process (Lemma 1)
  - Guarantee the convergence of our iterative training procedure (Proposition 1)

#### A.4 SCALING UP THE SYSTEM

To extend our framework to larger systems, we implement a hierarchical structure where clusters of Coordinator LLMs and their associated Execution LLMs form local Nash Equilibria, which are then coordinated through a global Coordinator LLM to establish a global Nash Equilibrium. This hierarchical design preserves our theoretical guarantees while enabling efficient scaling. The process is detailed in Algorithm 2.

---

**Algorithm 2** Scaling-Up Framework for EcoNash

**Require:** Global Coordinator LLM  $\text{Coord}_{\text{global}}$ , Local Coordinator LLMs  $\text{Coord}_k$ ,  $k = 1^K$

**Require:** System parameters  $\epsilon_C$ ,  $R_{\text{threshold}}$ ,  $\epsilon_L$ , Learning rates  $\eta, \eta', \eta_{\text{global}}$

**Ensure:** Optimized hierarchical Nash Equilibrium

- 1: Initialize cluster embeddings  $\mathbf{E}_{kk} = 1^K$  and prompt embeddings  $\mathbf{e}_i$  for all LLMs
- 2: **while** not converged **do**
- 3:    $\mathbf{S} \leftarrow \text{Coord}_{\text{global}}(\mathbf{e}_t)$  ▷ Global strategy generation
- 4:   **for** each cluster  $k = 1$  to  $K$  **in parallel do**
- 5:      $O_k \leftarrow [\mathbf{e}_t, \mathbf{S}, \mathbf{E}_k]^\top$  ▷ Cluster observation
- 6:     Local strategy:  $\mathbf{s}_k \leftarrow \text{Coord}_k(O_k)$
- 7:     **for** each Execution LLM  $i \in C_k$  **in parallel do**
- 8:        $O_i \leftarrow [\mathbf{e}_t, \mathbf{s}_k, \mathbf{b}_i]^\top$  ▷ Agent observation
- 9:       Generate output  $u_i$  with parameters  $(T_i, p_i)$
- 10:       Compute rewards:
- 11:          $r_i^{\text{AL}} \leftarrow \min(R_{\text{max}}, \text{sim}(u_i, c_k))$
- 12:          $r_i^{\text{TS}} \leftarrow \min(R_{\text{max}}, \text{eval}(u_i, \text{task}))$
- 13:          $r_i^{\text{CC}} \leftarrow \min(R_{\text{max}}, \text{quality}(u_i, u_j, j \in C_k))$
- 14:          $r_i \leftarrow \alpha_1 r_i^{\text{AL}} + \alpha_2 r_i^{\text{TS}} + \alpha_3 r_i^{\text{CC}}$
- 15:         Update belief network using loss  $L_i(\theta_i^B)$
- 16:     **end for**
- 17:      $c_k \leftarrow \text{Coord}_k(u_i, i \in C_k)$  ▷ Local commitment
- 18:     Update cluster embedding  $\mathbf{E}_k$  using local metrics
- 19:   **end forCopy**
- 20:    $C \leftarrow \text{Coord}_{\text{global}}(\{c_k\}_{k=1}^K)$  ▷ Global commitment
- 21:   **for** each cluster  $k = 1$  to  $K$  **do**
- 22:     Compute global reward:  $R_k \leftarrow R_{\text{global}}(\text{sim}(c_k, C))$
- 23:     Update local Coordinator parameters
- 24:   **end for**
- 25:   **Early Stopping Check:**
- 26:   **if**  $\|C_{t+1} - C_t\| \leq \epsilon_C$  **and**  $\frac{1}{K} \sum_{k=1}^K R_k \geq R_{\text{threshold}}$  **then**
- 27:     **break**
- 28:   **end if**
- 29: **end while**

1026

## A.4.1 DETAILED EXPLANATION

1027

1028

**Initialization**

1029

1030

1031

1032

1033

1034

1035

1036

1037

1038

1039

1040

1041

- **Clustering:** Execution LLMs are divided into  $K$  clusters  $\{C_1, C_2, \dots, C_K\}$  based on task similarity.
- **Local Coordinator LLMs:** Each cluster  $C_k$  is assigned a local Coordinator LLM  $\text{Coord}_k$  to manage its Execution LLMs.
- **Global Coordinator LLM:** A Central LLM  $\text{Central}$  oversees all clusters.
- **Embeddings:** Initialize prompt embeddings  $\mathbf{e}_i$  for Execution LLMs and cluster embeddings  $\mathbf{E}_k$  for clusters.

**Global Strategy Generation** The global Coordinator LLM generates a high-level strategy  $\mathbf{S}$  based on the question  $q$ . This strategy provides overall guidance and is distributed to all local Coordinator LLMs.

1041

1042

1043

1044

1045

**Local Inference and Optimization** Each local Coordinator LLM  $\text{Coord}_k$  generates a local strategy  $\mathbf{s}_k$  using  $\mathbf{S}$  and the cluster embedding  $\mathbf{E}_k$ . Execution LLMs within the cluster receive  $(q, \mathbf{s}_k, \mathbf{e}_i)$  and generate individual answers  $a_i$ . The local Coordinator LLM aggregates these answers to form a local commitment  $c_k$ .

1046

1047

1048

1049

**Local Optimization** Execution LLMs compute local rewards based on the similarity between their answers and the local commitment. Prompt embeddings  $\mathbf{e}_i$  are updated to maximize expected rewards. Cluster embeddings  $\mathbf{E}_k$  are also updated to improve Coordinator at the cluster level.

1050

1051

1052

**Global Commitment Formation** The global Coordinator LLM aggregates local commitments  $\{c_k\}$  to form the final global commitment  $C$ , representing the system's overall response.

1053

1054

1055

1056

**Global Optimization** Each cluster receives a global reward  $R_k$  based on the similarity between its local commitment  $c_k$  and the global commitment  $C$ . Local Coordinator LLMs are updated based on the global rewards to improve alignment with the global objective.

1057

1058

1059

1060

**Convergence Check** The system checks if global convergence criteria are met, such as minimal changes in the global commitment or reaching a performance threshold. If met, the algorithm terminates; otherwise, it proceeds to the next episode.

1061

## A.5 PROOF OF MIXING NETWORK MONOTONICITY

1062

1063

**Proposition 2** (Monotonicity of Mixing Network). *The mixing network  $Q_{tot}$  is monotonic in each individual Q-value  $Q_i$ , ensuring that improvements in  $Q_i$  lead to improvements in  $Q_{tot}$ .*

1064

1065

1066

1067

*Proof.* The mixing network is designed using positive weights and non-decreasing activation functions. Specifically, let the mixing network be composed of layers where each layer  $l$  computes:

1068

1069

1070

$$h^l = \phi^l(W^l h^{l-1} + b^l)$$

1071

where:

1072

1073

1074

1075

1076

1077

- $h^0 = [Q_1, Q_2, \dots, Q_N]^\top$
- $W^l$  has non-negative entries.
- $\phi^l$  is a non-decreasing activation function (e.g., ReLU).

1078

We proceed by induction to show that each component of  $h^l$  is a non-decreasing function of  $Q_i$ .

1079

**Base Case:** At layer  $l = 0$ ,  $h_i^0 = Q_i$ , so  $\frac{\partial h_i^0}{\partial Q_j} = \delta_{ij} \geq 0$ .

1080   **Inductive Step:** Assume  $\frac{\partial h_k^{l-1}}{\partial Q_i} \geq 0$  for all  $k$ . Then, for each component  $h_j^l$ :

$$1083 \quad h_j^l = \phi^l \left( \sum_k W_{jk}^l h_k^{l-1} + b_j^l \right)$$

1086   Since  $W_{jk}^l \geq 0$  and  $\phi^l$  is non-decreasing:

$$1089 \quad \frac{\partial h_j^l}{\partial Q_i} = \phi'^l \left( \sum_k W_{jk}^l h_k^{l-1} + b_j^l \right) \sum_k W_{jk}^l \frac{\partial h_k^{l-1}}{\partial Q_i} \geq 0$$

1092   because  $\phi'^l \geq 0$  and  $\frac{\partial h_k^{l-1}}{\partial Q_i} \geq 0$  by the inductive hypothesis. Therefore,  $\frac{\partial Q_{\text{tot}}}{\partial Q_i} \geq 0$ , ensuring  
1093   monotonicity.  $\square$

1095

1096   This monotonicity property is crucial as it ensures that improvements in individual agent perfor-  
1097   mances contribute positively to the overall system performance, aligning local and global objectives  
1098   within EcoNash.

1099

## 1100   B DETAILED PROOFS

### 1102   B.1 PROOF OF LEMMA 1

1104   *Proof.* Consider the value functions under policies  $\pi'$  and  $\pi$ :

$$1106 \quad V_i^{\pi'}(s) = \mathbb{E}_{\pi'} \left[ \sum_{k=0}^{\infty} \gamma^k r_i(s_k, a_k) \mid s_0 = s \right], \quad V_i^{\pi}(s) = \mathbb{E}_{\pi} \left[ \sum_{k=0}^{\infty} \gamma^k r_i(s_k, a_k) \mid s_0 = s \right].$$

1109   Their difference is:

$$1111 \quad V_i^{\pi'}(s) - V_i^{\pi}(s) = \mathbb{E}_{\pi'} \left[ \sum_{k=0}^{\infty} \gamma^k r_i(s_k, a_k) \right] - \mathbb{E}_{\pi} \left[ \sum_{k=0}^{\infty} \gamma^k r_i(s_k, a_k) \right]$$

$$1114 \quad = \sum_{k=0}^{\infty} \gamma^k \left( \mathbb{E}_{s_k \sim d_{\pi'}^k} [r_i(s_k, a_k)] - \mathbb{E}_{s_k \sim d_{\pi}^k} [r_i(s_k, a_k)] \right).$$

1116   Assuming the difference in state distributions is negligible (justified under Assumption 4), we focus  
1117   on action differences. Using the Q-function definition:

$$1119 \quad Q_i^{\pi}(s, a_i, a_{-i}) = r_i(s, a_i, a_{-i}) + \gamma \mathbb{E}_{s' \sim P} [V_i^{\pi}(s')],$$

1121   we can write:

$$1122 \quad V_i^{\pi'}(s) - V_i^{\pi}(s) = \sum_{k=0}^{\infty} \gamma^k \mathbb{E}_{s_k \sim d_{\pi'}^k} [Q_i^{\pi}(s_k, a'_k) - V_i^{\pi}(s_k)].$$

1124   Since  $V_i^{\pi}(s_k) = \mathbb{E}_{a_k \sim \pi(s_k)} [Q_i^{\pi}(s_k, a_k)]$ , we have:

$$1127 \quad V_i^{\pi'}(s) - V_i^{\pi}(s) = \sum_{k=0}^{\infty} \gamma^k \mathbb{E}_{s_k \sim d_{\pi'}^k} \left[ \mathbb{E}_{a'_k \sim \pi'(s_k)} [Q_i^{\pi}(s_k, a'_k) - \mathbb{E}_{a_k \sim \pi(s_k)} [Q_i^{\pi}(s_k, a_k)]] \right].$$

1129   Switching the order of expectations and summing over  $k$ , we get:

$$1131 \quad V_i^{\pi'}(s) - V_i^{\pi}(s) = \frac{1}{1-\gamma} \mathbb{E}_{s \sim d_{\pi'}} [Q_i^{\pi}(s, a'_i, a'_{-i}) - Q_i^{\pi}(s, a_i, a_{-i})].$$

1133

$\square$

1134 B.2 BOUNDING THE BAYESIAN REGRET  
11351136 Starting from the regret definition for agent  $i$  over  $T$  steps:

1137 
$$1138 R_i(T) = \mathbb{E}_{s_t, \pi_t} \left[ \sum_{t=1}^T (V_i^*(s_t) - V_i^{\pi_t}(s_t)) \right],$$
  
1139

1140 where the expectation is over the randomness in state transitions and policies.  
1141

1142 Applying Lemma 1:

1143 
$$1144 V_i^*(s_t) - V_i^{\pi_t}(s_t) = \frac{1}{1-\gamma} \mathbb{E}_{a_i^{*t}, a_{-i}^{*t}, a_i^t, a_{-i}^t} [Q_i^{\pi_t}(s_t, a_i^{*t}, a_{-i}^{*t}) - Q_i^{\pi_t}(s_t, a_i^t, a_{-i}^t)].$$
  
1145

1146 We decompose the Q-value difference:

1147 
$$1148 Q_i^{\pi_t}(s_t, a_i^{*t}, a_{-i}^{*t}) - Q_i^{\pi_t}(s_t, a_i^t, a_{-i}^t) \\ 1149 = (Q_i^{\pi_t}(s_t, a_i^{*t}, a_{-i}^{*t}) - Q_i^*(s_t, a_i^{*t}, a_{-i}^{*t})) \quad (\text{Error Term 1}) \\ 1150 + (Q_i^*(s_t, a_i^{*t}, a_{-i}^{*t}) - Q_i^*(s_t, a_i^t, a_{-i}^t)) \quad (\text{Policy Suboptimality}) \\ 1151 + (Q_i^*(s_t, a_i^t, a_{-i}^t) - Q_i^{\pi_t}(s_t, a_i^t, a_{-i}^t)). \quad (\text{Error Term 2})$$
  
1152

1153 Define the Q-function estimation error:

1154 
$$1155 \epsilon_t = \max_{s, a_i, a_{-i}} |Q_i^{\pi_t}(s, a_i, a_{-i}) - Q_i^*(s, a_i, a_{-i})|.$$

1156 **Assumption 5** (Q-function Estimation Error). *The estimation error decreases as:*

1157 
$$1158 \epsilon_t \leq \frac{C_\epsilon}{t^\alpha}, \quad \text{with } \alpha = \frac{1}{2}.$$
  
1159

1160 This rate is justified by:

- 1161 • Stochastic approximation theory showing
- $O(t^{-1/2})$
- convergence (Borkar (2009)).
- 
- 1162
- 
- 1163 • Minimax optimality in stochastic optimization (Nemirovski et al. (2009)).
- 
- 1164
- 
- 1165 • Achievement through proper learning rate scheduling.

1166 **Assumption 6** (Policy Suboptimality). *The policy suboptimality decreases as:*

1167 
$$1168 \delta_t \leq \frac{C_\delta}{t^\beta}, \quad \text{with } \beta = \frac{1}{2}.$$
  
1169

1170 This rate is supported by:

- 1171 • Regret bounds in online learning (Hazan (2016)).
- 
- 1172
- 
- 1173 • Gradient-based methods in convex policy spaces (Shalev-Shwartz (2012)).
- 
- 1174
- 
- 1175 • Empirical evidence in cooperative multi-agent RL (Zhang et al. (2021)).

1176 Using these assumptions, we have:

1177 
$$1178 Q_i^{\pi_t}(s_t, a_i^{*t}, a_{-i}^{*t}) - Q_i^{\pi_t}(s_t, a_i^t, a_{-i}^t) \leq 2\epsilon_t + \delta_t.$$

1179 Summing over  $t$  and all agents:

1180 
$$1181 R(T) \leq \sum_{i=1}^N \frac{1}{1-\gamma} \sum_{t=1}^T (2\epsilon_t + \delta_t) \\ 1182 \leq \sum_{i=1}^N \frac{1}{1-\gamma} \left( 2C_\epsilon \sum_{t=1}^T \frac{1}{t^\alpha} + C_\delta \sum_{t=1}^T \frac{1}{t^\beta} \right) \\ 1184 \\ 1185 \\ 1186 \\ 1187 = O\left(\frac{N\sqrt{T}}{1-\gamma}\right).$$

1188 B.3 COMPARISON WITH MULTI-AGENT DEBATE  
11891190 In multi-agent debate settings, we analyze the regret bound using the same decomposition from  
1191 Lemma 1:1192 **Assumption 7** (Persistent Policy Suboptimality in Debate).

1193 
$$\delta_t \geq \delta_{\min} > 0$$

1194 Justified by:

- 1195
- 1197 • Game-theoretic properties of competitive settings Fudenberg & Levine (1998)
  - 1198 • Information-theoretic limitations Owe & Sims (2013)
  - 1200 • Empirical evidence of non-convergence Lanctot et al. (2017)

1201 Following the same decomposition from earlier:

1202 
$$V_i^*(s_t) - V_i^{\pi_t}(s_t) = \frac{1}{1-\gamma} \mathbb{E}_{a_i, a_{-i}} [Q_i^{\pi_t}(s_t, a_i^{*t}, a_{-i}^{*t}) - Q_i^{\pi_t}(s_t, a_i^t, a_{-i}^t)]$$

1203 The Q-value difference still decomposes into three terms:

1204 
$$\begin{aligned} & Q_i^{\pi_t}(s_t, a_i^{*t}, a_{-i}^{*t}) - Q_i^{\pi_t}(s_t, a_i^t, a_{-i}^t) \\ &= \underbrace{(Q_i^{\pi_t}(s_t, a_i^{*t}, a_{-i}^{*t}) - Q_i^*(s_t, a_i^{*t}, a_{-i}^{*t}))}_{\leq \epsilon_t} \\ &\quad + \underbrace{(Q_i^*(s_t, a_i^{*t}, a_{-i}^{*t}) - Q_i^*(s_t, a_i^t, a_{-i}^t))}_{\geq \delta_{\min}} \\ &\quad + \underbrace{(Q_i^*(s_t, a_i^t, a_{-i}^t) - Q_i^{\pi_t}(s_t, a_i^t, a_{-i}^t))}_{\leq \epsilon_t} \end{aligned}$$

1205 In the debate setting:

- 1206
- 1208 • The estimation error terms are still bounded by  $\epsilon_t = \frac{C_\epsilon}{\sqrt{t}}$
  - 1209 • The policy suboptimality term is lower bounded by  $\delta_{\min}$  (Assumption 7)

1210 Therefore, for each agent  $i$ :

1211 
$$\begin{aligned} R_i(T) &= \mathbb{E} \left[ \sum_{t=1}^T (V_i^*(s_t) - V_i^{\pi_t}(s_t)) \right] \\ &\leq \frac{1}{1-\gamma} \sum_{t=1}^T (2\epsilon_t + \delta_{\min}) \\ &= \frac{1}{1-\gamma} \left( 2C_\epsilon \sum_{t=1}^T \frac{1}{\sqrt{t}} + \delta_{\min} T \right) \\ &\leq \frac{1}{1-\gamma} \left( 2C_\epsilon \cdot 2(\sqrt{T} - 1) + \delta_{\min} T \right) \end{aligned}$$

1212 Summing over all agents and noting that the  $\delta_{\min} T$  term dominates:

1213 
$$R_{\text{debate}}(T) = O \left( \frac{N \delta_{\min} T}{1-\gamma} \right)$$

1214 This linear growth contrasts with our framework's sublinear  $O(N\sqrt{T})$  bound, demonstrating  
1215 EcoNash's superior efficiency through coordinated learning toward BNE.

1242

## B.4 DETAILED REWARD SETTING

1243

The reward function  $R$  provides feedback on each agent's performance while respecting Assumption 1, ensuring all reward components are uniformly bounded by  $R_{\max}$ . Drawing inspiration from maximum entropy inverse reinforcement learning (Zhu et al., 2023), we define the Action Likelihood Reward  $r_i^{\text{AL}} = \min(R_{\max}, \text{sim}(u_i, C))$ , where  $\text{sim}(u_i, C) = \frac{u_i \cdot C}{\|u_i\| \|C\|}$  measures the consistency between an agent's output  $u_i$  and the coordinator's commitment  $C$ . Following Hao et al. (2023), the Task-Specific Reward  $r_i^{\text{TS}} = \min(R_{\max}, \text{eval}(u_i, \text{task}))$  evaluates domain-specific objectives through the coordinator's assessment, where eval computes normalized scores considering solution correctness in mathematical problems or response relevance in planning tasks. Building upon Xie et al. (2024b), the Collaborative Contribution Reward  $r_i^{\text{CC}} = \min(R_{\max}, \text{quality}(u_i, \{u_j\}_{j \neq i}))$  enables the coordinator to assess each agent's output quality within the multi-agent context, where quality evaluates the response's coherence and creativity while considering its contribution to the collective solution. The total reward combines these components as  $r_i = \alpha_1 r_i^{\text{AL}} + \alpha_2 r_i^{\text{TS}} + \alpha_3 r_i^{\text{CC}}$ , where the weights  $\alpha_1 + \alpha_2 + \alpha_3 = 1$  ensure the total reward is bounded by  $R_{\max}$ . To enhance adaptability and learning efficiency, we introduce a dynamic mechanism to adjust these weights using gradient-based updates  $\alpha_k \leftarrow \alpha_k - \eta_\alpha \cdot \partial \mathcal{L}_{\text{dr}} / \partial \alpha_k$ , where  $\mathcal{L}_{\text{dr}} = \sum_{i=1}^N (r_i^{\text{actual}} - r_i^{\text{expected}})^2$  measures the discrepancy between actual and expected rewards.

1259

## B.5 TASK SETUPS

1260

GSM8K is a benchmark for mathematical reasoning that requires multi-step problem solving. Given a context description and a question, it requires step-by-step mathematical reasoning and computation to arrive at a final answer. The dataset contains approximately 7.5K problems in the training set and 1.3K problems in the test set. Problems range from basic arithmetic to complex word problems, testing both mathematical and logical reasoning capabilities.

1261

SVAMP is a challenging mathematical word problem dataset specifically designed to test the robustness of language models in solving arithmetic problems. It contains 1,000 elementary math word problems, carefully curated to probe for specific vulnerabilities in mathematical reasoning systems. The problems require understanding both mathematical concepts and natural language semantics, with a focus on structural variations that test genuine problem-solving capabilities rather than pattern matching.

1262

Strategy QA is a question answering dataset that focuses on multi-hop reasoning and strategic thinking. It consists of 2,290 yes/no questions, each requiring implicit multi-step reasoning and background knowledge to arrive at the correct answer. Unlike traditional QA datasets, Strategy QA questions cannot be answered by simply retrieving and combining explicit facts, making it an effective benchmark for testing complex reasoning capabilities.

1263

MATH is a comprehensive mathematics dataset spanning various topics from algebra to calculus. It contains approximately 12K problems across different difficulty levels, with detailed step-by-step solutions. The dataset is structured into multiple categories including algebra, counting and probability, geometry, intermediate algebra, number theory, prealgebra, and precalculus, making it particularly effective for evaluating mathematical problem-solving capabilities across different domains.

1264

GSM-Hard is a specialized subset of mathematical word problems specifically designed to test advanced reasoning capabilities. It contains problems that are significantly more challenging than standard GSM8K problems, requiring more complex multi-step reasoning and mathematical operations. The dataset focuses on problems that typically have lower success rates with standard approaches, making it particularly useful for evaluating the upper bounds of model performance.

1265

TravelPlanner is a benchmark crafted for evaluating language agents in tool-use and complex planning within multiple constraints. The dataset comprises 1,225 queries in total, divided into training (45 queries), validation (180 queries), and test (1,000 queries) sets. The benchmark incorporates three types of constraints: environment constraints for testing adaptability to real-world conditions, commonsense constraints for evaluating practical reasoning, and hard constraints for assessing the ability to satisfy specific user requirements such as budget limitations. This structure makes TravelPlanner particularly effective for evaluating both reasoning capabilities and practical planning skills in real-world scenarios.

1296 B.6 HYPERPARAMETER  
12971298 Table 8: Hyperparameters of EcoNash  
1299

Parameter	Value	Description
<b>Training Configuration</b>		
Episodes per Task	100	Number of episodes per task
Buffer Size	32	Size of on-policy buffer
Batch Size	16	Mini-batch size for training
Update Interval	8	Policy update frequency (episodes)
Optimizer	Adam	Optimization algorithm
Learning Rate ( $\eta$ )	0.001	Learning rate for execution LLMs
Learning Rate ( $\eta_{\text{coord}}$ )	0.0005	Learning rate for coordinator LLM
Discount Factor ( $\gamma$ )	0.99	Discount factor for future rewards
<b>Network Architecture</b>		
Entity Dimension ( $d$ )	256	Dimension of entity embeddings
Belief State Dimension ( $d_b$ )	128	Dimension of belief state
Attention Heads ( $H$ )	4	Number of attention heads
MLP Hidden Size	256	Hidden layer size in belief encoder
Transformer Blocks	2	Number of transformer layers
Key/Query Dimension	64	Dimension per attention head ( $d/H$ )
Feed-forward Size	1024	Dimension of FFN intermediate layer
Dropout Rate	0.1	Dropout probability in attention
Layer Norm Epsilon	$1 \times 10^{-5}$	Layer normalization parameter
<b>Temperature and Sampling Control</b>		
$T_{\min}$	0.1	Minimum temperature value
$T_{\max}$	2.0	Maximum temperature value
$p_{\min}$	0.1	Minimum sampling parameter
$p_{\max}$	0.9	Maximum sampling parameter
<b>Reward Configuration</b>		
$R_{\max}$	1.0	Maximum reward bound
$\alpha_1$ (AL weight)	0.4	Action Likelihood reward weight
$\alpha_2$ (TS weight)	0.4	Task-specific reward weight
$\alpha_3$ (SE weight)	0.2	Self-Evaluation reward weight
<b>Loss Weights</b>		
$\lambda_b$	0.1	Weight for belief network loss
$\lambda$	0.1	Regularization weight in encoder
$\lambda_m$	0.1	Weight for mixing network consistency
<b>Early Stopping</b>		
$\epsilon_C$	0.01	Commitment change threshold
$\epsilon_L$	$1 \times 10^{-4}$	Loss convergence threshold
$R_{\text{threshold}}$	0.7	Average reward threshold
$T_{\text{patience}}$	5	Patience epochs for validation
<b>Model Size</b>		
Learnable Parameters	$\sim 1.7M$	Total trainable parameters

1344

1345

1346

1347

1348

1349

1350  
 1351  
 1352  
 1353  
 1354  
 1355  
 1356  
 1357  
 1358  
 1359  
 1360  
 1361  
 1362  
 1363  
 1364  
 1365  
 1366  
 1367  
 1368  
 1369  
 1370  
 1371  
 1372     **C PROMPT**  
 1373  
 1374     **D EXAMPLE**  
 1375  
 1376         **D.1 CASE STUDY**  
 1377  
 1378  
 1379  
 1380  
 1381  
 1382  
 1383  
 1384  
 1385  
 1386  
 1387  
 1388  
 1389  
 1390  
 1391  
 1392  
 1393  
 1394  
 1395  
 1396  
 1397  
 1398  
 1399  
 1400  
 1401  
 1402  
 1403

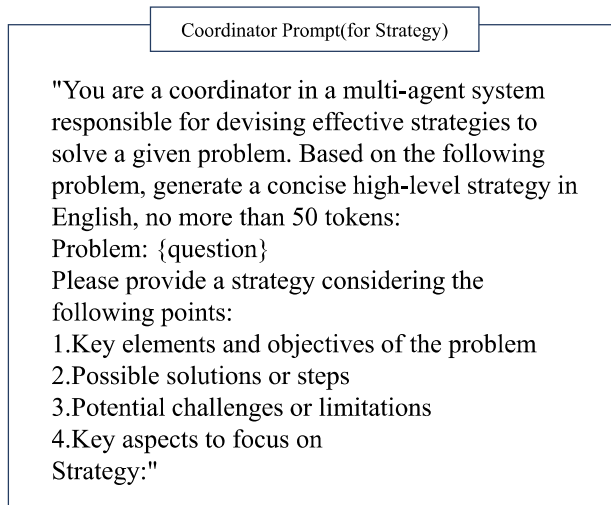


Figure 4: Coordinator Prompt(for Strategy)

1404  
 1405  
 1406  
 1407  
 1408  
 1409  
 1410  
 1411  
 1412  
 1413  
 1414  
 1415  
 1416  
 1417  
 1418  
 1419  
 1420  
 1421  
 1422  
 1423  
 1424  
 1425  
 1426  
 1427  
 1428  
 1429  
 1430  
 1431  
 1432  
 1433  
 1434  
 1435  
 1436  
 1437  
 1438  
 1439  
 1440  
 1441  
 1442  
 1443  
 1444  
 1445  
 1446  
 1447  
 1448  
 1449  
 1450  
 1451  
 1452  
 1453  
 1454  
 1455  
 1456  
 1457

Coordinator Prompt(for Commitment)

"You are a coordinator in a multi-agent system responsible for reviewing the answers of multiple execution LLMs based on a given strategy. Your tasks are:

1. Form a Commitment: Integrate the best aspects of all answers to ensure consistency in the solution process and accuracy in the final result.
2. Evaluate each answer: Assess the similarity of the solution process to the Commitment and the accuracy of the final result. Based on these criteria, assign a reward score between 0 and 1 to each answer.

Strategy: {strategy}

Execution LLMs' Answers:

- LLM1: {answer1}
- LLM2: {answer2} ...
- LLMn: {answern}

Please follow these steps: a. Review each LLM's answer to determine its adherence to the strategy and the correctness of the solution. b. Formulate a comprehensive Commitment by integrating the most effective methods and accurate results from the answers. c. Evaluate each answer based on the following criteria:

- Process Similarity: The consistency of the solution steps with the Commitment
- Result Accuracy: The correctness of the final answer Assign a reward score between 0 and 1 to each LLM, where 1 means full adherence to the Commitment and completely correct results, and 0 means no adherence or incorrect results.

Please output the results in the following structured format:

Commitment: {Detail the integrated solution here, including key steps and the final result}

Evaluation and Rewards:

- LLM1: {score1} (Brief explanation for the score no more than 10 tokens)
- LLM2: {score2} (Brief explanation for the score no more than 10 tokens)
- ...
- LLMn: {scoren} (Brief explanation for the score no more than 10 tokens)

Figure 5: Coordinator Prompt(for Commitment)

1458  
 1459  
 1460  
 1461  
 1462  
 1463  
 1464  
 1465  
 1466  
 1467  
 1468  
 1469  
 1470  
 1471  
 1472  
 1473  
 1474  
 1475  
 1476  
 1477  
 1478  
 1479  
 1480  
 1481  
 1482  
 1483  
 1484  
 1485  
 1486  
 1487  
 1488  
 1489  
 1490  
 1491  
 1492  
 1493  
 1494  
 1495  
 1496  
 1497  
 1498  
 1499  
 1500  
 1501  
 1502  
 1503  
 1504  
 1505  
 1506  
 1507  
 1508  
 1509  
 1510  
 1511

Execution LLM

"You are an execution LLM in a multi-agent system, responsible for deriving solutions based on a given strategy and your own belief network. Each LLM has different beliefs but cannot access the outputs of other LLMs. Your tasks are:

1. Form your belief based on the strategy: Assume other LLMs will follow certain potential solutions. Your goal is to generate the optimal solution without global information.
2. Output the best answer: Considering your belief about other LLMs' outputs, derive the optimal solution for the current environment.
3. Bayesian Nash Equilibrium: Your output should maximize expected utility under incomplete information, aligning with the strategy.
4. Feedback adjustment: Ensure your solution is coherent under uncertainty and optimized for the best result.

Strategy: {strategy}

Please follow these steps: a. Review the strategy and form your belief on how other LLMs might output. b. Based on your belief, derive and output your optimal solution. c. Ensure your solution aligns with Bayesian Nash Equilibrium, maximizing expected utility.

Final answer:"

Figure 6: Execution LLM

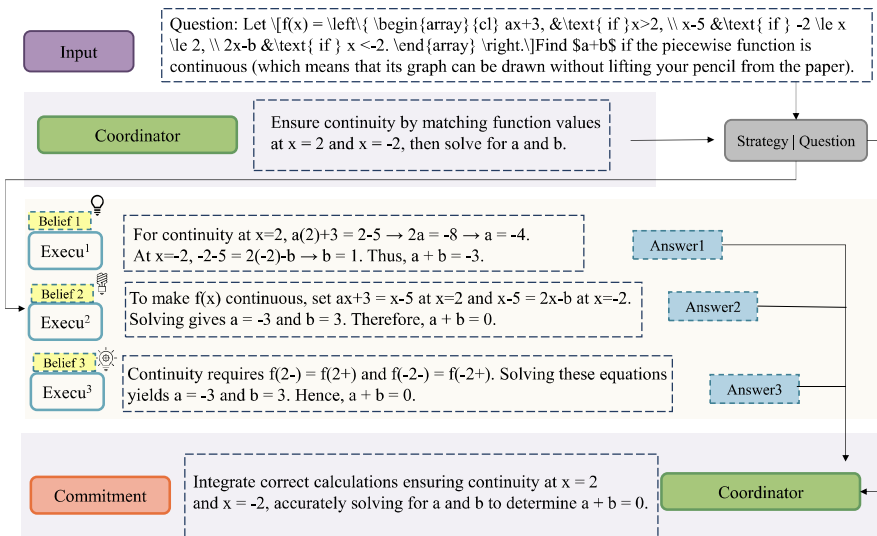


Figure 7: case study of math

## D.2 STRATEGY EXAMPLE

### D.2.1 GSM8K

**Q1:** John buys 3 pizzas for \$12 each. If he gives the delivery person a 20% tip on the total, how much did he spend in total?

**S1:** Calculate pizza subtotal first. Add 20% of subtotal for tip. Sum for final amount.

**F1:**

1. Pizza cost = \$? \times ?

- 1512        2. Tip = ?  $\times$  subtotal  
 1513        3. Total = subtotal + tip  
 1514

1515 *Strategy + Format : 35tokens*

1517 **Q2:** Janet saves twice as much money as Tom. If Tom saves \$45 per week, how much does Janet  
 1518 save in 5 weeks?

1520 **S2:** Find Janet's weekly savings relative to Tom's. Multiply by number of weeks.

1522 **F2:**

- 1524        1. Janet weekly = ?  $\times$  Tom  
 1525        2. Total = weekly  $\times$  weeks  
 1526

1527 *Strategy + Format : 28tokens*

1529 **Q3:** A factory produces 150 cars per day. If they increase production by 15% next month, how  
 1530 many cars will they produce in a 30-day month?

1532 **S3:** Calculate production increase. Add to original. Multiply by days in month.

1534 **F3:**

- 1535        1. Increase = original  $\times$  15%  
 1536        2. New daily = original + increase  
 1538        3. Monthly = daily  $\times$  days  
 1539

1540 *Strategy + Format : 36tokens*

1542 **Q4:** Alex has 240 marbles and gives  $\frac{3}{8}$  of them to Sarah. Sarah then gives  $\frac{1}{4}$  of her marbles to  
 1543 Tom. How many marbles does Sarah have left?

1545 **S4:** Calculate Sarah's initial share. Find amount she gives to Tom. Subtract.

1547 **F4:**

- 1548        1. Sarah gets = total  $\times$   $\frac{3}{8}$   
 1549        2. Sarah gives = her marbles  $\times$   $\frac{1}{4}$   
 1551        3. Remaining = initial - given  
 1552

1553 *Strategy + Format : 39tokens*

1555 **Q5:** A train travels at 60 mph for 2.5 hours, then increases speed to 75 mph for 1.5 hours. What's  
 1556 the total distance traveled?

1558 **S5:** Calculate distance for each speed separately using  $d = r \times t$ . Sum distances.

1560 **F5:**

- 1561        1. First distance = speed<sub>1</sub>  $\times$  time<sub>1</sub>  
 1562        2. Second distance = speed<sub>2</sub>  $\times$  time<sub>2</sub>  
 1564        3. Total =  $d_1 + d_2$   
 1565

1565 *Strategy + Format : 36tokens*

1566 D.2.2 MATH  
 1567

1568 **Q1:** In a bag of marbles,  $\frac{3}{7}$  are blue and  $\frac{2}{5}$  are red. The remaining 11 marbles are green. How  
 1569 many marbles are in the bag?

1570  
 1571 **S1:** Convert fractions to common denominator. Find the fraction for remaining color. Use given  
 1572 count to find total.

1573  
 1574 **F1:**

- 1575     1. Convert to common denominator  
 1576     2. Add converted fractions  
 1577     3. Subtract from whole  
 1578     4. Use remaining count to find total

1581 *Strategy + Format : 32tokens*  
 1582

1583 **Q2:** Find the area of a triangle with vertices at (0,0), (4,0), and (2,5).

1584  
 1585 **S2:** Use coordinate geometry method for area. Set up calculation matrix. Take final result.

1587 **F2:**

- 1588     1. Set up coordinate matrix  
 1589     2. Calculate determinant  
 1590     3. Apply area formula

1593 *Strategy + Format : 28tokens*  
 1594

1595 **Q3:** If  $\log_2(x) = 3$  and  $\log_2(y) = 4$ , find  $\log_2(xy)$ .

1596  
 1597 **S3:** Apply logarithm properties. Combine given values. Express final result.

1599 **F3:**

- 1600     1. Write multiplication property  
 1601     2. Substitute given values  
 1602     3. Simplify result

1605 *Strategy + Format : 26tokens*  
 1606

1607 **Q4:** A circle has radius 6. Find the area of the sector formed by a  $40^\circ$  angle at the center.

1609  
 1610 **S4:** Convert angle measurement. Apply sector area formula. Simplify result.

1611 **F4:**

- 1612     1. Convert to radians  
 1613     2. Write sector formula  
 1614     3. Calculate final area

1617 *Strategy + Format : 27tokens*  
 1618

1619 **Q5:** Solve the equation:  $2x^2 + 5x - 12 = 0$ .

1620     **S5:** Identify quadratic components. Apply standard formula. Solve for variables.  
 1621

1622     **F5:**  
 1623

- 1624       1. Identify coefficients  
 1625       2. Setup quadratic formula  
 1626       3. Calculate solutions  
 1627

1629     *Strategy + Format : 28tokens*  
 1630

1631     D.2.3   SVAMP  
 1632

1633     **Q1:** There are 56 books on the shelf. Tom puts 14 more books and Jane removes 22 books. How  
 1634       many books are on the shelf now?  
 1635

1636     **S1:** Track sequential changes. Apply additions and subtractions in order.  
 1637

1638     **F1:**  
 1639

- 1640       1. Add new books  
 1641       2. Subtract removed books  
 1642

1643     *Strategy + Format : 25tokens*  
 1644

1645     **Q2:** A box has 3 rows of chocolates. Each row has 4 chocolates. If 5 chocolates were eaten, how  
 1646       many are left?  
 1647

1648     **S2:** Calculate initial total. Subtract consumed amount.  
 1649

1650     **F2:**  
 1651

- 1652       1. Find total chocolates  
 1653       2. Subtract eaten ones  
 1654

1656     *Strategy + Format : 23tokens*  
 1657

1658     **Q3:** Mary has 5 times as many stickers as John. John has 12 stickers. How many stickers do they  
 1659       have together?  
 1660

1661     **S3:** Calculate second person's amount. Sum both quantities.  
 1662

1663     **F3:**  
 1664

- 1665       1. Find Mary's stickers  
 1666       2. Add both totals  
 1667

1668     *Strategy + Format : 24tokens*  
 1669

1670     **Q4:** A garden has 35 flowers. ( $\frac{2}{7}$ ) are roses and ( $\frac{3}{7}$ ) are tulips. How many flowers are neither roses  
 1671       nor tulips?  
 1672

1673     **S4:** Sum known fractions. Find remaining fraction. Calculate final count.

1674

**F4:**

1675

1676

1. Add type fractions
2. Find remaining fraction
3. Calculate flower count

1678

*Strategy + Format : 27tokens*

1681

1682

**Q5:** Each child needs 3 pencils. If there are 23 children, how many boxes of 10 pencils should the teacher buy?

1684

**S5:** Calculate total need. Convert to required units. Round appropriately.

1686

**F5:**

1688

1689

1. Calculate total pencils
2. Divide by box size
3. Round to whole boxes

1692

*Strategy + Format : 28tokens*

1694

**Note on Token Counts:**

1696

1697

- All problems now follow consistent format: strategy + step-by-step format
- Strategy statements aim to be concise yet clear
- Format points provide framework without giving solutions
- Token ranges:
  - Shortest: 23 tokens (SVAMP Q2)
  - Longest: 39 tokens (GSM8K Q4)
  - Average: (~)30 tokens

1699

1700

1701

1702

1703

1704

1705

1706

1707

1708

1709

1710

1711

1712

1713

1714

1715

1716

1717

1718

1719

1720

1721

1722

1723

1724

1725

1726

1727